Western Kentucky University

TopSCHOLAR®

Masters Theses & Specialist Projects | Graduate School

Fall 2020

Novel Application of Graphene Oxide Based-Biosensor Utilizing CRISPR/dCas9 for Rapid Detection of Antibiotic Resistance Genes

Joel Omage
Western Kentucky University, joel.omage178@topper.wku.edu

Follow this and additional works at: https://digitalcommons.wku.edu/theses

 Part of the Biochemical and Biomolecular Engineering Commons, Life Sciences Commons, and the Medicine and Health Sciences Commons

Recommended Citation

Omage, Joel, "Novel Application of Graphene Oxide Based-Biosensor Utilizing CRISPR/dCas9 for Rapid Detection of Antibiotic Resistance Genes" (2020). *Masters Theses & Specialist Projects.* Paper 3467.
https://digitalcommons.wku.edu/theses/3467

This Thesis is brought to you for free and open access by TopSCHOLAR®. It has been accepted for inclusion in Masters Theses & Specialist Projects by an authorized administrator of TopSCHOLAR®. For more information, please contact topscholar@wku.edu.

NOVEL APPLICATION OF GRAPHENE OXIDE BASED-BIOSENSOR UTILIZING CRISPR/DCAS9 FOR RAPID DETECTION OF ANTIBIOTIC RESISTANCE GENES

A Thesis
Presented to
The Faculty in the Department of Chemistry
Western Kentucky University
Bowling Green, Kentucky

In Partial Fulfillment
Of the Requirements for the Degree
Master of Science

By
Joel Imoukhuede Omage

December 2020

NOVEL APPLICATION OF GRAPHENE OXIDE
BASED-BIOSENSOR UTILIZING CRISPR/DCAS9
FOR RAPID DETECTION OF ANTIBIOTIC RESISTANCE GENES

Date Recommended 11/19/2020

Moon-Soo Kim Digitally signed by Moon-Soo Kim
Date: 2020.11.20 13:01:54 +09'00'

Dr. Moon-Soo Kim, Director of Thesis

Kevin M. Williams, Ph.D. Digitally signed by Kevin M. Williams, Ph.D.
Date: 2020.11.19 18:59:48 -06'00'

Dr. Kevin Williams

Ajay Srivastava Digitally signed by Ajay Srivastava
Date: 2020.11.19 20:56:52 -06'00'

Dr. Ajay Srivastava

Associate Provost for Research and Graduate Education

This thesis is dedicated to my Parents, Mr. Robert Omage and Mrs. Mabel Omage for their continual support and prayers for me.

ACKNOWLEDGEMENTS

I like to thank and appreciate my research advisor, Dr. Moon-Soo Kim, for her consistent guidance, and support throughout my graduate program at WKU. Under her mentorship, I acquired fundamental training in biomedical research and useful skills in Chemistry, which are invaluable to pursue my career path in medical and chemical research.

In addition, I am very grateful to my thesis committee members, Dr. Kevin Williams and Dr. Ajay Srivastava for their time, proof reading and evaluating my thesis. Also, I thank Ji Young Shim (PhD), and Colleen Jackson for their time and effort in training me as well as other members of Dr. Kim's lab who contributed to my research in different capacity and at various times during my graduate program. They include Cecil Wendy, Narayan Neupane and Nguyen Van (PhD).

Finally, I am grateful to the Department of Chemistry and Graduate School, WKU, Department head, Dr. Kevin Williams and other faculty members for their training, support and the opportunity they provided to me throughout the program.

CONTENTS

LIST OF FIGURES

LIST OF TABLES

NOVEL APPLICATION OF GRAPHENE OXIDE
BASED-BIOSENSOR UTILIZING CRISPR/DCAS9
FOR RAPID DETECTION OF ANTIBIOTIC RESISTANCE GENES

Joel Omage December 2020 49 Pages

Directed by: Moon-Soo Kim, Kevin Williams, and Ajay Srivastava

Department of Chemistry Western Kentucky University

Antibiotic resistance is one of the biggest public health challenges globally. To combat this threat, we have designed a method for the facile and rapid detection of antibiotic resistance gene (ARG) in bacteria. We utilized an emerging tool termed the clusters of regularly interspaced short palindromic repeats (CRISPR) in complex with deactivated CRISPR associated proteins (dCas9) on conjugated 2-dimensional graphene oxide (GO) sheets. Nuclease-deactivated Cas9 in complex with customized single guided RNA (sgRNA) was used for the target DNA recognition. The sgRNA was easy to design and we demonstrated that it is complementary to its target sequence by performing a Cas9 cleavage assay. The sgRNA was then successfully labelled with Alexa-488 dye. The GO was immobilized with anti-CRISPR Cas9 antibody and its surface morphology was characterized by Atomic Force Microscopy (AFM) to confirm the successful immobilization of the antibody to the GO. Our approach is based on the fluorescence quenching mechanism of antibody-GO in the absence and presence of target DNA. It was then validated by performing a sensitivity assay to detect the specific dsDNA within the tetM gene using the labelled-sgRNA/dcas9 ribonucleoprotein. The CRISPR complex was adsorbed onto the GO surface via the Cas9 antibody immobilized to the GO. In the absence of target DNA, fluorescence signal of the labeled sgRNA/dCas9 was quenched due to fluorescence resonance energy transfer (FRET) between Alexa fluorophore and GO when

they are in close proximity. However, in the presence of target DNA, the bound dcas9/sgRNA-DNA complex was dissociated from the GO, restoring the fluorescence signal. The detection limit of the tetM gene was as low as 1 nM. This novel detection approach has the potential to be further developed and applied at the point-of-care (POC) for antibiotic resistant bacteria detection.

CHAPTER I – INTRODUCTION

1. Antibiotic Resistant Gene (ARG)

The WHO recognizes antibiotic resistance as a major global health threat (WHO 2014) because it causes hundreds of thousands of deaths annually.[1] Traditionally, the fight against antibiotic resistance is aimed at the clinical, community and recently agricultural settings in order to treat and prevent transmission of antibiotic resistant bacteria.[1] The environment is well recognized as a source of antibiotic resistance but there is no clear understanding of how the antibiotic resistance develops.[2,3] This makes it difficult to mitigate the emergence and dissemination of antibiotic resistance, an indicator for the urgent need to develop mitigation strategies.[1,4] According to the operational definition of resistance, a strain is resistant against an antibiotic if its minimal inhibitory concentration (MIC) is higher than the corresponding parental wild-type strain.[5] A resistance gene allows a bacterium strain to survive a higher antibiotic concentration or reduces the susceptibility of a bacterium strain towards a specific antibiotic.[1] Resistant genes, especially novel resistant genes, may remain unknown until perhaps they result in clinical problems, which might be difficult to manage unless they are identified rapidly.[1] Novel antibiotic resistance genes could emerge from any of the astounding number of bacterial cells on earth via genetic variability, mutations, rearrangements and horizontal gene transfer (Fig 1).[1] However, a lot of studies have been conducted for the facile and rapid detection of ARG using the early PCR-based approach, DNA-binding proteins and CRISPR/Cas proteins.[6,7,8,9,10].

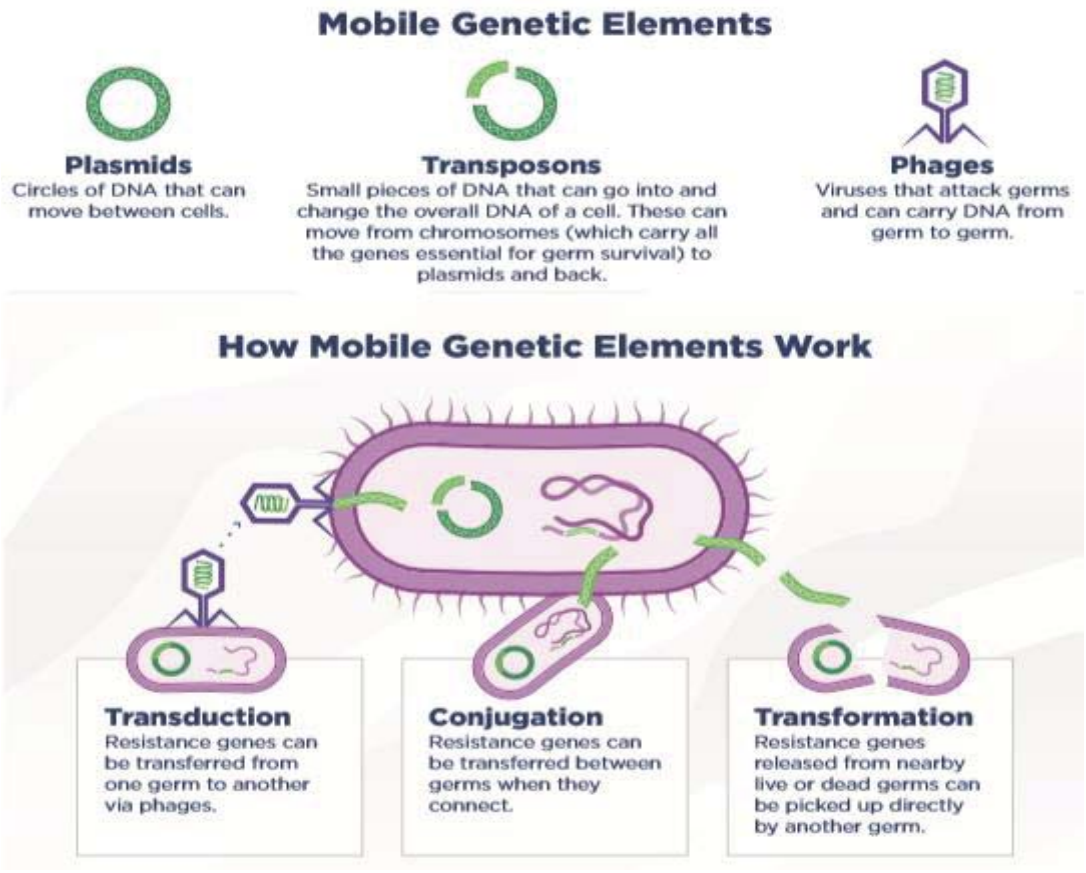

Figure 1: Horizontal transfer of antibiotic resistance gene. (Centers for Disease Control and Prevention- https://www.cdc.gov/drugresistance/pdf/threats-report/How-AR-Moves-508.pdf).

2. **Polymerase Chain Reaction (PCR)-Based Technology**

The PCR tool has been widely used in the amplification and detection of nucleic acids in clinical samples such as blood.[7] This has allowed for the broad analysis and identification of biomarkers such as antibiotic resistant gene indicative of various pathogen infections.[11] Analytical data from the PCR afford physicians with specific information to improve patient outcomes and introduce specific medical treatment.[11] Although there is significant advancement in nucleic acid detection, the PCR nucleic acid detection tool is

time consuming and expensive to use, as it requires multi-step reactions, several reagents, and skilled personnel. Moreover, the PCR amplification technique often requires the complex design and optimization procedures of probes/primers for efficient targeting. In addition, the optical components for detection in the PCR technique are large and costly.[11] Thus, an innovative approach is desirable to overcome the drawbacks associated with traditional PCR-based nucleic acid strategies. This will enable us to provide low-cost and portable compact nucleic acid-based analytical tools to expand their clinical utility.[11] The emergence of programmable double stranded DNA binding domains creates an alternative diagnostic tool that avoids the time consuming and tedious steps involved in PCR-based techniques.[11,12]

3. DNA-binding Proteins

3.1 Zinc Finger Proteins (ZFPs)

Zinc fingers (ZFs) are the most common DNA-binding domains. In eukaryotes, Cys2-His2 (C2H2) domain is the most common type of DNA-binding motif, which consists of multiple cysteine and histidine residues in a total of about 30 amino acids.[8] The ZF-motif is stabilized by Zn^{2+} ions bounded to two cysteine and two histidine ligands.[8] Each finger recognizes selectively 3-4 DNA nucleotides because each amino acid in a ZF has an affinity for a specific nucleotide. Hence, for DNA detection, a tandem of six ZF modules can be designed to recognize as many as 18 base pairs of DNA sequence and effectively used for diagnostic purposes.[8]

3.2 Transcription activator-like effectors (TALEs)

Another type of DNA-binding domain is TALE (Transcription Activator-Like Effectors)-domains. TALEs are also modular proteins that can be designed to target a specific DNA sequence. Each repeat in TALEs recognizes only one nucleotide unlike a ZF-domain that binds three nucleotide bases.[12] The binding of a TALE protein to its specific nucleotide is determined by two hypervariable amino acids known as repeat variable di-residues (RVDs) within the repeat domain of 34 amino acid residues.[8] The sum of repeats and the sequences of RVDs determine the length and the target nucleotide composition that would be recognized by TALE proteins. By decoding the TALE RVD code, engineering TALEs with the high target specificity and selectivity has been made possible.[8] TALE-proteins can specifically target dsDNA, RNA-DNA hybrids, including retroviral RNAs hybridized to specific capturing DNA.[7]

4. CRISPR-Cas System and Its Applications

The CRISPR (clustered regularly interspaced short palindromic repeats) and Cas (CRISPR-associated) proteins are adaptive immune systems utilized by most archaea and bacterial cells as defense against foreign DNA or RNA.[16] The CRISPR/Cas system makes use of an antisense RNA as memory signature for previous viral nucleic acid invasion. A CRISPR locus is made up of a CRISPR array of short direct repeats (diverse Cas genes) interspaced by short variable DNA sequences (called 'spacers').[13] The mechanism of CRISPR–Cas adaptive immunity comprises three distinct phases: adaptation, expression and interference.[13] The adaptation process involves the acquisition of foreign fragments of invading viral or plasmid DNA (known as 'protospacers') into the CRISPR array. These

new spacers provide recognition sequences for targeted destruction of subsequent viral or plasmid DNA. During the expression stage, the CRISPR array undergoes transcription and maturation processes for the synthesis of a precursor transcript (pre-crRNA), which later matures into a CRISPR RNA (crRNA). During the interference stage, the association of crRNA and Cas proteins form a CRISPR-Cas endonuclease for the specific targeting and cleavage of cognate viruses or plasmids DNA.[13] Usually, in many CRISPR–Cas systems, recognition of a short protospacer adjacent motif (PAM) in the target DNA, is required prior to protospacer acquisition.[13]

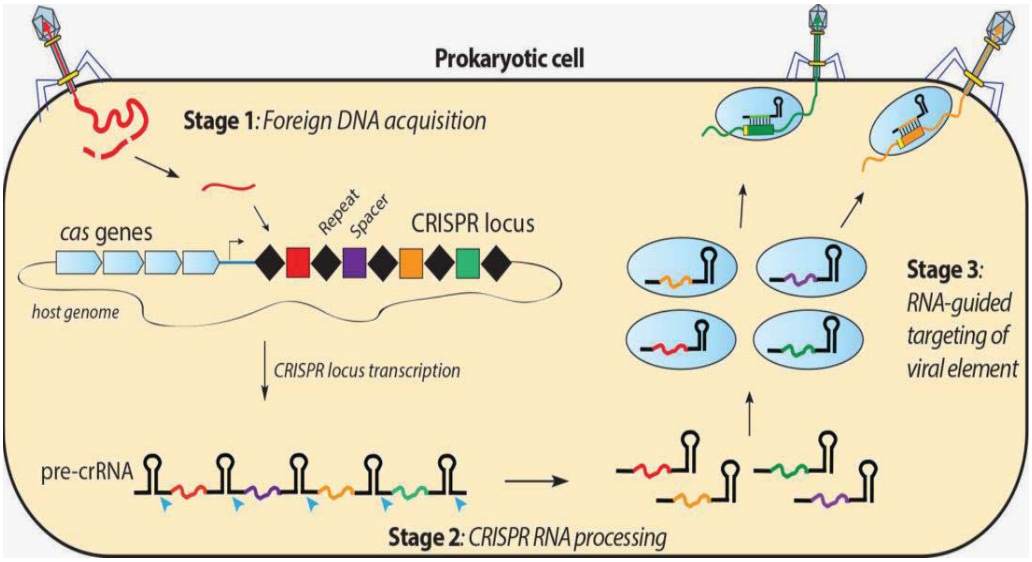

Figure 2: CRISPR/Cas9 adaptive immune system.[11]

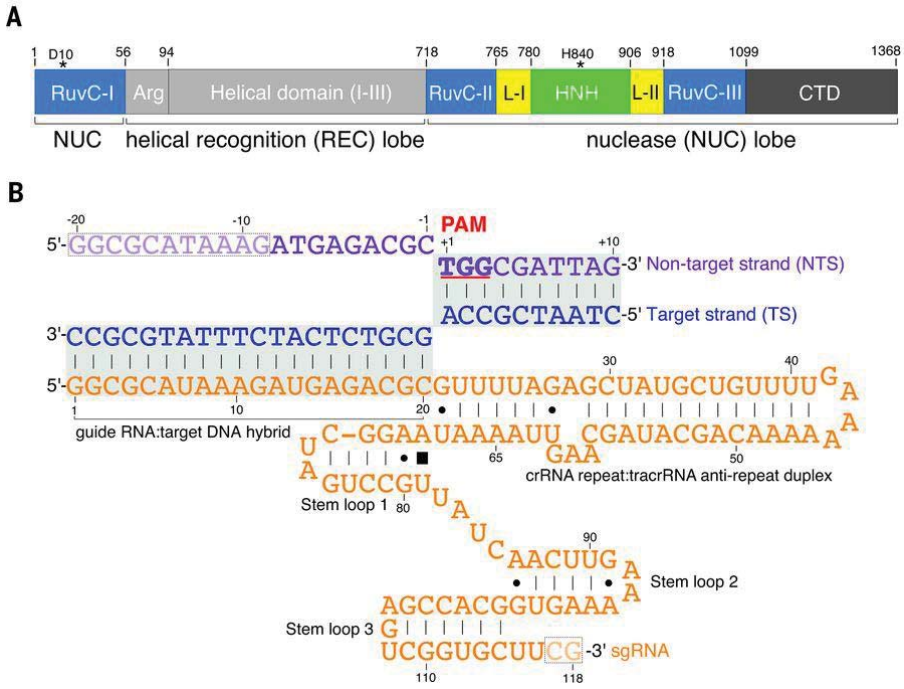

Figure 3: (A) Domain organization of S. pyogenes Cas9.[14] (B) Schematic diagram of the sgRNA–target DNA complex.[14]

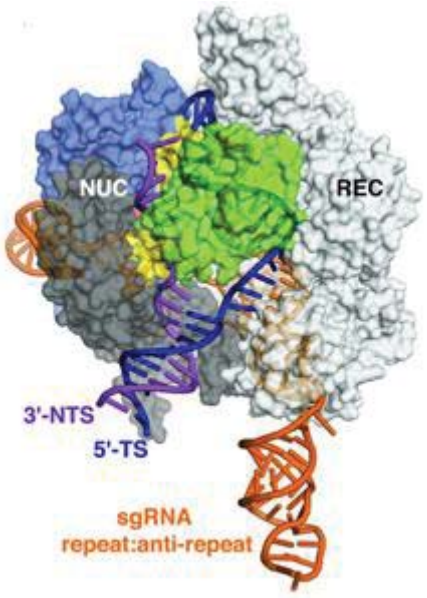

Figure 4: Surface representations of the Cas9-sgRNA-dsDNA structure.[14]

4.1 CRISPR-dCas9 for the Detection of Antibiotic Resistant Bacteria

The CRISPR/Cas system is a major tool employed for the rapid and early detection of antibiotic resistant bacteria or pathogens to aid therapeutic treatment.[15,16] A CRISPR/dCas9-mediated biosensor that combines a catalytically inactivated or dead Cas9 (dCas9) and single microring resonator (SMR) biosensor based-isothermal nucleic acid amplification was used for the rapid and highly sensitive detection of two tick-borne pathogens that have substantial overlapping clinical presentations: *Orientia tsutsugamushi*, the causative agent of Scrub typhus (ST), and Bunyavirus, the causative agent of severe fever with thrombocytopenia syndrome (SFTS).[10] This diagnostic tool clearly distinguished ST from SFTS within 20 min in serum samples. Another pathogen detection based on an isothermal tool for amplifying and detecting- double stranded DNA, known as CRISPR-Cas9-triggerd nicking endonuclease-mediated Strand Displacement Amplification method (CRISDA).[17] This method takes advantage of the high sensitivity, specificity and unique conformational rearrangements of CRISPR effectors in recognizing the target DNA.[17] The CRISDA is used with a peptide nucleic acid (PNA) invasion - mediated endpoint measurement, which displays attomolar sensitivity and specificity in detection of different DNA targets under a complex sample background. CRISDA shows sub-attomolar sensitivity when combined with a Cas9-facilitated target approach.[17] Thus, it is a powerful isothermal tool for the ultrasensitive and specific detection of DNA sequence in point-of-care (POC) diagnostics and field analyses. Mengqi and colleagues also applied CRISPR/Cas9 triggered isothermal amplification for site-specific detection using a real-time fluorescence monitoring method.[18] An exponential amplification reaction strategy was combined to CRISPR/Cas (CAS-EXPAR) in their study. It was demonstrated

that this strategy gave a detection limit in the attomolar range and showed excellent specificity in discriminating single-base mismatches.[18] The applicability of this method was verified to detect DNA methylation and the total RNA of L. monocytogenes.[18] Similarly, the CRISPR effector Cas13a also known as C2c2, was used as a rapid, inexpensive, and sensitive nucleic acid detection and could be used at a point-of-care (POC) pathogen detection, genotyping, and disease monitoring.[19] The effect of Cas13a was combined with isothermal amplification to develop a CRISPR-based diagnostic (CRISPR-Dx) for rapid DNA or RNA detection with attomolar sensitivity and single-base mismatch specificity.[19] A detection platform known as specific high-sensitivity enzymatic reporter unlocking (SHERLOCK), was used to detect specific strains of Zika and Dengue virus, pathogenic bacteria as well as genotype human DNA and to identify mutations in cell-free tumor DNA.[19] Using the CRISPR-mediated DNA FISH method, a complex of nuclease activity-deactivated Cas9 protein and sgRNA was employed to rapidly and reliably diagnose methicillin-resistant Staphylococcus aureus (MRSA). This diagnosis is critical for guiding effective patient treatment and preventing the spread of MRSA infections.[20] SYBR Green l was used as a fluorescent probe to detect the gene within 30 min with high sensitivity without requiring a gene separation step using cell lysates.[20]

5. Fluorescence Resonance Energy Transfer-based Detection

Fluorescent technology is widely used today in medical diagnosis for its essential sensitivity and high selectivity.[21] There are several fluorescent biosensors including the ratiometric fluorescent biosensor which records florescence intensity at two wavelengths simultaneously. It has an advantage over other fluorescent biosensors because it produces better quantitative florescence signal.[22] The two strategies of ratiometric fluorescent

biosensors are intra-molecular charge transfer (ICT) and Förster resonance energy transfer-based approach.[21] For the ICT, the accuracy of biosensors could be altered by the interactions between targets and the biosensor or spectrum broadening. However, due to the single excitation and longer emission in Florescence Resonance Energy Transfer (FRET), it doesn't suffer same limitation as in ICT.[21] Most biosensors for biomedical applications are based on the FRET because of its non-invasive and real-time florescence signal that changes with the characteristics of the fluorophore.[23] In addition to being fast, sensitive and specific, FRET-based biosensors also have facile and homogeneous assay for quantitative measurements.[21]

5.1 Principle of FRET

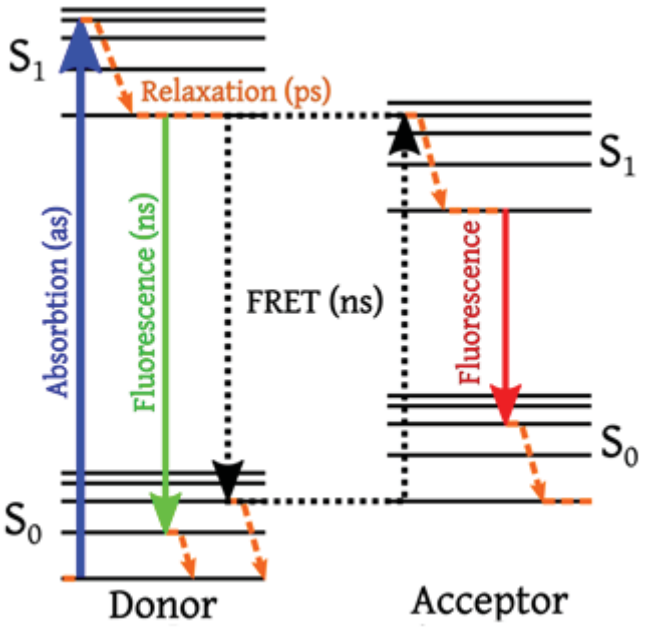

Figure 5. Principle of FRET[21]

FRET occurs when two photosensitive molecules donate and accept energy. The donor fluorophore, initially in its electronically excited state, transfers energy to an

acceptor chromophore as shown in Figure 5.[21] The FRET efficiency (E) depends on 1) the spectral overlap (J) of the donor emission spectrum and the acceptor absorption spectrum, 2) the distance between the donor and the acceptor (typically in the range of 1–10 nm), and 3) the relative orientation of the donor emission dipole moment and the acceptor absorption dipole moment. Traditionally, in FRET, one donor (D) is combined with one acceptor (A).[21] For such a single pair of fluorophores, the efficiency (E) of FRET is inversely proportional to the sixth power of the distance between donor and acceptor, making FRET extremely sensitive to small changes in distance (r) between the donor and the acceptor. Recently, many biosensors based on nanomaterials have been designed in which multiple acceptors are attached to a single donor or vice versa.[21]

5.2 FRET donor and acceptor

Most commercial fluorophores can be available as FRET donors or acceptors. Examples of organic donors include dyes such as pyrene-based analogue, and cyanine-(Cy3.5, Cy5.5) rhodamine.[21] Some of these organic dyes require conjugation onto functionalized-polymeric microspheres by using functionalized groups such as biotin, avidin, amines, sulfates, and carboxylates to increase the fluorescent signal for targets, or are modified to increase their water-solubility.[21] Examples of FRET acceptors (Quenchers) include many organics such as 4-(4′- dimethylaminophenylazo) benzoic acid (Dabcyl) and metallic materials for instance gold nanoparticles due to their broad absorption spectra.[21] Fluorescent proteins (FPs) such as green fluorescent protein (GFP), and blue florescent protein (BFP) have also been served as tags of the donor or acceptor for monitoring protein-protein interactions or conformational changes of individual proteins in living cells.[24] In addition, fluorescent nanoparticles including quantum dots (QDs) and carbon dots (CDs)

with broad absorption can serve as both donor and acceptor.[25] The structure of linker space and property of fluorophore pair could also affect the intrinsic FRET efficiency of the probe.[21]

5.3 Analysis of FRET data

FRET is generally detected by an appropriate fluorescence spectrometer or microscope equipment, either as a decrease in the donor (D) fluorescence intensity, or as an increase in the acceptor (A) fluorescence intensity upon excitation or a resultant effect of both.[21] A variable in the FRET signal known as A/D FRET ratio was introduced and it is a measure of the amount of targets, where the maximal fluorescent intensity of the acceptor and donor are denoted by A and D respectively.[26] In FRET analysis, the crosstalk of spectrum between the donor and acceptor could be a major challenge. This means a possible overlap can ensue between the donor and acceptor emission and excitation wavelengths. However, fluorophores such as quantum dots that exhibit large stoke shifts can minimize crosstalk.[21] Also, fluorophores with long florescence half-lives, such as lanthanide chelate dyes, have been shown to eliminate interfering florescence in time-resolved FRET assays. In addition, the crosstalk can also be eliminated indirectly by the mathematical introduction of a second excitation and emission wavelengths or utilizing correction parameters.[21] It is also possible to obtain spatial data and optical information utilizing fluorescent imaging based on FRET.[21]

5.4 FRET-based Sensors with Graphene Oxide

The two-dimensional nano sheet graphene oxide (GO) (Fig 6) represents a new type of solution dispersible, non-stoichiometric macromolecule that can complex with many

organic and inorganic systems, making GO an attractive tunable platform for optical applications.[27] The presence of carboxylic acid, epoxy and hydroxyl groups around the edges and on the basal planes of GO allows for its chemical modification.[28] Although GO is fluorescent, it has the ability to quench fluorescence from fluorophores adsorbed on its surface such as dyes and quantum dots.[27] Studies indicate this quenching effect originates from FRET, or non-radiative dipole–dipole coupling between the fluorescent species and GO.[27] The presence of ionic groups and aromatic domains around the planes and edges of GO allow electrostatic interactions with charged proteins and DNA and provides a platform for p–p stacking and quenching of dyes.[27] This quenching ability of GO makes it suitable as an optical biosensor device for detecting nucleic acids and biomolecules.[27] Most GO-based biosensor have been utilized for ssDNA detection.[27]

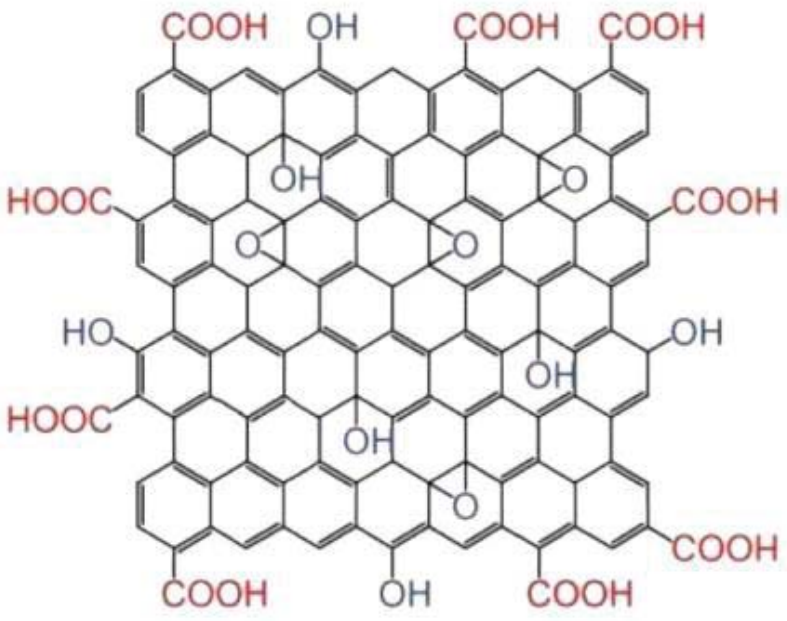

Figure 6: Structure of Graphene Oxide.[29]

Jinghong Li group in 2010 developed an aptasensor for thrombin detection based on FRET.[30] The bio sensing platform was constructed by conjugating dye labeled DNA-aptamer on graphene. This is possible due to the noncovalent assembly induced by π-π stacking of DNA bases on graphene. The fluorescence quenching of FAM dye- labeled aptamers by graphene and subsequent fluorescence recovery induced by thrombin was monitored and evaluated by florescence spectra. In 2017, Tianming Yao research group created an immune-sensing platform based on FRET principle for the detection of proteins in a buffer solution.[31] This biosensor was constructed by conjugating antibodies to GO for the quantitative determination of protein analytes. In the presence of analyte proteins and standard fluorescein-labeled proteins, which compete for the binding sites, the analyte concentration can be obtained based on the quantitative florescence quenching of fluorescein-labelled proteins by GO. Hence, upon increasing the amount of analyte protein concentration, there was a direct increase in fluorescence intensity measured from the unquenched fluorescein-labeled proteins. This biosensor serves as an alternative to enzyme-linked immunosorbent assay (ELISA).

6. Aims of Study

The goal of this study is to develop, utilize and validate a CRISPR-mediated GO-FRET method for direct detection of dsDNA. The use of CRISPR technology for diagnosis is growing rapidly due to its high selectivity and specificity with minimal off-target effects compared to other methods such as those utilizing DNA-binding proteins. The CRISPR assay involves the use of a Cas protein and a single guide RNA (sgRNA) that is complementary to target DNA in base pairs. In this study, we will utilize a catalytically dead CRISPR associated (dCas9) protein because target DNA is not needed to be cleaved.

Several studies have already successfully utilized dCas9/sgRNA complex ribonucleoprotein as a detection probe for targeted DNA.[20,32] However, our approach utilizes a detection method different from the previous reports. Also, no study has combined FRET-GO technology with the CRISPR technology. We believe that we would demonstrate for the first time a facile and rapid detection of dsDNA using GO-FRET biosensor immobilized with dCas9/sgRNA complex. First, we will express and purify the dcas9 protein and design a single guide RNA complementary to the target DNA. Afterwards, we will label the designed sgRNA with an appropriate fluorophore such as Alexa dye to form sgRNA-Alexa and combine it with dcas9 to form dCas9/sgRNA-Alexa complex. Next, we will synthesize a GO-conjugated dcas9 antibody that will allow for immobilization of the ribonucleoprotein (RNP) onto the GO surface via peptide bond formation. We expect that the GO, as an electron acceptor, will quench the florescence from the RNP. However, upon adding target dsDNA, the RNP interacts more with the target dsDNA and dissociates farther from the GO to bring about florescence recovery. The florescence can be quantitatively measured as our detection method. Therefore, multiple sgRNAs will be synthesized to develop and validate the CRISPR-mediated GO-FRET method for direct detection of dsDNA.

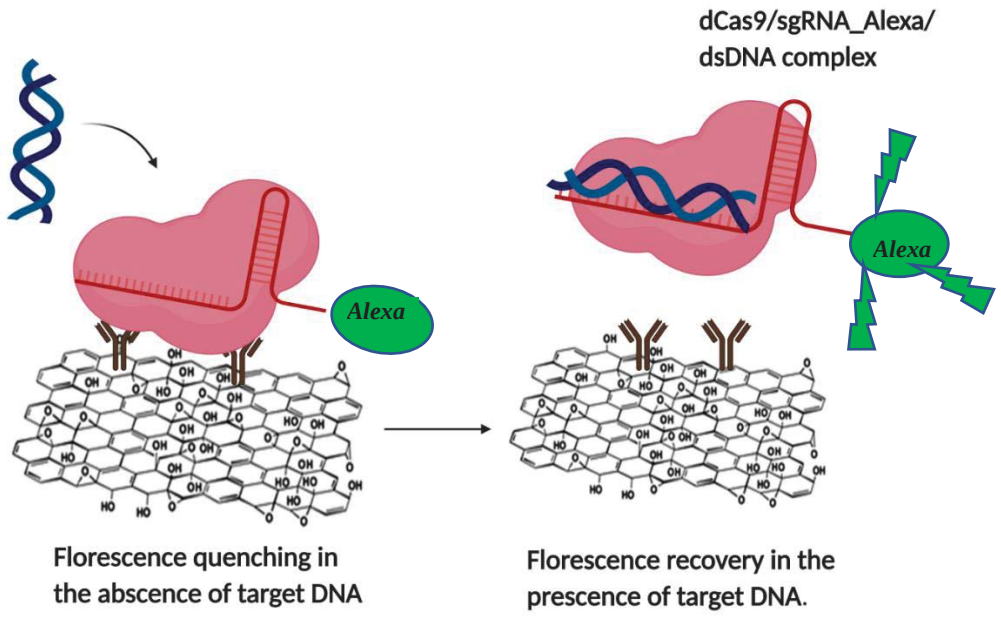

Figure 7: Schematic diagram of dCas9/sgRNA assay with Ab-GO

CHAPTER II – EXPERIMENTAL

1. Expression and Purification of dCas9 Protein

The pET-dCas9 plasmid purchased from Genscript (Piscataway, New Jersey) was transformed into the *E. coli* BL21 Rosetta 2 (DE3). Cells were grown at 37 °C in LB medium containing 50 μg/ml ampicillin until the optical density at 600 nm (OD600) reached 0.6. Protein expression was induced by supplementing with 0.5 mM isopropyl-1-thio-β-D-galactopyranoside (IPTG) for 16 h at 16 °C and 250 rpm. After harvesting the cell by centrifugation, the pellets were resuspended in lysis buffer (20 mM HEPES pH 7.5, 300 mM NaCl, 25 mM Imidazole, 0.5 mM TCEP and 1mM protease inhibitor cocktail (Roche)). The cell lysate was sonicated and the soluble protein was obtained by centrifugation for 1 h at 16,000g, applied to Ni-NTA agarose resin (Thermofisher) in a column already equilibrated with the lysis buffer. The cell lysate was washed twice with the lysis buffer and eluted with buffer (20 mM Tris–HCl, 0.5 M NaCl, 0.5 M Imidazole, pH 8.0). The purified proteins were pooled together and further purified by using the 100kDa Amicon centrifugal filter.

2. Design of sgRNA

We designed multiple 20-nt sgRNA using a CRISPR design online tool called Benchling. This tool helps to design sgRNAs and provide specificity and efficiency scores to screen out sgRNA with high off target effects. Five sgRNAs (Table 1) with high specificity and efficiency were selected based on their relatively high on- and off- target scores. Four of the sgRNA designed are complementary to the tetracycline resistant gene (tetM) non-template strand while only one targets the template strand. For higher targeting

efficiency, the sgRNA is manually designed to bind to the non-template DNA strand of the target sequence.[33] If the template DNA strand of the coding sequence is targeted, the efficiency of the CRISPR system is generally low, at best leading to mild repression (~50 %).[34]

In addition to the 20-bp base pairing region, the sgRNA 20-nt sequence was designed to be complementary to a 20-nt sequence on the target DNA that is adjacent to a protospacer adjacent motif (PAM) sequence. Each of the sgRNA was designed to require 5′ NGG as PAM motif on both target and non- target strands for recognizing a 20-nt region in the tetM gene.

Staphylococcus aureus strain 2952 tetracycline resistance protein TetM (tetM) gene, partial cds

GenBank: AY057894.1

AGTTTTAGCTCATGTTGATGCGGGAAAAACTACCTTAACAGAAAGCTTATTATATAACAGTGGAGCGATT
ACAGAATTAGGAAGCGTGGACAAAGGTACAACGAGGACGGATAATACGCTTTTAGAACGTCAGAGAGG
AATTACAATTCAGACAGGAATAACCTCTTTTCAGTGGGAAAATACGAAGGTGAACATCATAGACACGCC
AGGACATATGGATTTCTTAGCAGAAGTATATCGTTCATTATCAGTTTTAGATGGGGCAATTCTACTGATTT
CTGCAAAAGATGGCGTACAAGCACAAACTCGTATATTATTTCATGCACTTAGGAAAATGGGGATTCCCAC
AATCTTTTTTATCAATAAGATTGACCAAAATGGAATTGATTTATCAACGGTTTATCAGGATATTAAAGAG
AAACTTTCTGCCGAAATTGTAATCAAACAGAAGGTAGAACTGTATCCTAATGTGTGTGTGACGAACTTTA
CCGAATCTGAACAATGGGATACGGTAATAGAGGGAAACGATGACCTTTTAGAGAAATATATGTCCGGTA
AATCATTAGAAGCATTGGAACTCGAACAAGAGGAAAGCATAAGATTTCAGAATTGTTCTCTGTTCCCTCT
TTATCATGGAAGTGCAAAAAGTAATATAGGGATTGATAACCTTATAGAAGTGATTACGAATAAATTTTAT
TCATCAACACATCGAGGTCAGTCTGAACTTTGCGGAAATGTTTTCAAAATTGAATATACAAAAAAAAGAC
AACGTCTTGCATATATACGTCTTTATAGTGGCGTACTGCATTTGCGAGATTCGGTTAGAATATCGGAAAA
GGAAAAAATAAAAATTACAGAAATGTATACTTCAATAAATGGTGAATTATGTAA**AATCGATAAGGCTTA**
TTCCGGGGAAATTGTTATTTTGCAAAATGAGTTTTTGAAGTTAAATAGTGTTCTTGGAGATACAAAACTA
TTGCCACAGAGAAAAAAGATTGAAAATCCGCACCCTCTACTACAAACAACTGTTGAACCGAGTAAACCT
GAACAGAGAGAAATGTTGCTTGATGCCCTTTTGGAAATCTCAGATAGTGA**TCCGCTTCTACGATATTAC**
GTGGATTCTACGACACATGAAATTATACTTTCTTTCTTAGGGAAAGTACAAATGGAAGTGATTAGTGCAC
TGTTGCAAGAAAAGTATCATGTGGAGATAGAACTAAAAGAGCCTACAGTCATTTATATGGAGAGACCGT
TAAAAAATGCAGAATATACCATTCACATCGAAGTGCCGCCAAATCCTTTCTGGGCTTCCATTGGTTTA**TC**
TGTATCACCGCTTCCGTTGGGAAGTGGAATGCAGTATGAGAGCTCGGTTTCTCTTGGATACTTAAATCA
ATCATTTCAAAATGCA**GTTATGGAAGGGATACGCTA**TGGCTGTGAACAAGGATTGTATGGTTGGAATGT

GACGGACTGTAAAATCTGTTTTAAGTATGGCTTATACTATAGCCCTGTTAGTACCCCAGCAGATTTTCGGA
TGCTTGCTCCTATTGTATTGGAACAAGTCTTAAAAAAAGCTGGAACAGAATTGTTAGAGCCATATCTTAG
TTTTAAAATTTATGCGCCACAGGAATATCTTTCACGAGCATACAACGATGCTCCTAAATATTGTGCGAAC
ATCGTAGACACTCAATTGAAAAATAATGAGGTCATTCTTAGTGGAGAAATCCCTGCTCGGTGTATTCAAG
AATATCGTAGTGATTTAACTTTCTTTACAAATGGACGTAGTGTTTGTTTAACAGAGTTAAAAGGGTACCAT
GTTACTACCGGTGAACCTGTTTGCCAGCCCCGTCGTCTAAATAGTCGGA

Figure 8: tetM gene Template strand showing the 20-nt sequences of custom designed sgRNAs.

Table1: The five selected base pairing regions of custom designed sgRNAs on both template and non-template strands.

T1	TCCGCTTCTACGATATTACG
T2 (Non-Template Strand)	TCCACGTAATATCGTAGAAG
T3	TCTGTATCA*CCG*CTTCCGTT
T5	AATCGATAAGGCTTATT*CCG*
T6	GTTATGGAAGGGATACGCTA

2.1 Preparation of sgRNA

The DNA template for the target sgRNA was synthesized by designing a 56-to 58-nt forward PCR primer. The forward primer was designed to include the specific sgRNA target sequence (20 nt), which is between the Guide-it Scaffold Template-annealing sequence (15 nt at the 3'end of the primer) and a T7 promoter sequence plus four extra bases (21 nt in total) at the 5' end of the primer. A transcription initiation site (0–2 guanine (G) residues) was added dependent on the 5' end of the target sequence. The reason is that the T7 promoter requires at least two Gs for efficient transcription.

Table 2: PCR forward primer design to generate a DNA template for an sgRNA containing target sequence.

Extra bases (4bp)	T7 Promoter Sequence (17 bp)	G(s) added (0-2 bp)	Target sequence (20bp)	Scaffold_Template annealing sequence
CCTC	TAATACGACTCACTATA	GG	TCCGCTTCTACGATATTACG	GTTTAAGAGCTATGC
CCTC	TAATACGACTCACTATA	GG	TCCACGTAATATCGTAGAAG	GTTTAAGAGCTATGC
CCTC	TAATACGACTCACTATA	GG	TCTGTATCA*CCG*CTTCCGTT	GTTTAAGAGCTATGC
CCTC	TAATACGACTCACTATA	GG	AATCGATAAGGCTTATT*CCG*	GTTTAAGAGCTATGC
CCTC	TAATACGACTCACTATA	G	GTTATGGAAGGGATACGCTA	GTTTAAGAGCTATGC

2.2 Amplification of sgRNA Template

For the amplification of the sgRNA template (encoding template for sgRNA transcription), a 25 µL PCR mixture was prepared by combining 0.5 µL of the forward primer (10 µM) synthesized by IDT + 1 µL Guide-it Scaffold template + 12.5 µL PrimeSTAR Max premix + 11 µL RNase Free water in a 200 µL PCR tube. The single guide ribonucleic acid DNA template was amplified using a thermal cycler under the conditions from the Guide-it sgRNA in Vitro Transcription system (Takara Bio, California, USA) manufacturer's instructions. After amplification of the template, 5 µl of the PCR product was analyzed on a 1.2% agarose gel with a 100-bp DNA ladder.

2.3 In Vitro Transcription (IVT) Reaction

The PCR amplified product was directly used as template for the IVT reaction without purification. In a 200 µl PCR tube, a 20 µL mixture was combined, which contains 5 µl sgRNA PCR template+ 7 µl guide-it in vitro transcription buffer + 3 µL Guide-it T7 polymerase mix + 5 µl RNase free water. The mixture was vortexed and spun down to collect the reagents at the bottom of the tube and then placed in thermal cycler conditions

obtained from the Guide-it sgRNA in Vitro Transcription system (Takara Bio, California, USA) manufacturer's instructions. Following incubation, 2 µl of Recombinant DNase I (RNase-Free) was added to the 20 µl IVT reaction. Briefly, the reaction (22 µl) was vortexed and spun down to collect the reagents at the bottom of the tube. The reaction was then placed in a preheated thermal cycler with a heated lid according to the program conditions from the in vitro transcription kit manual - 33 cycles of; denaturation at 98 °C for 10 seconds and annealing at 60 °C for 10 seconds.

2.4 Purification of Transcribed sgRNA

The transcribed sgRNA was purified using the Guide-it IVT RNA Clean-Up Kit. Before purifying sgRNA, the IVT Wash Buffer was prepared by adding 24 ml of 96–100% ethanol and 78 µl of RNase free water to the reaction mixture for a total volume of 100 µl. All 100 µl was transferred to a 1.5-ml micro centrifuge tube. Then, 30 µl of IVT Binding Buffer + 130 µl of isopropanol were added and vortexed for 5 seconds after each addition. An IVT RNA clean-up spin column was placed in a collection tube and the sample was loaded onto the column for centrifugation at 11,000g for 30 seconds at room temperature. The flow through was discarded and the column was placed back in the Collection Tube. Again, 600 µl of IVT Wash Buffer was added and centrifuged at 11,000g for 30 seconds at room temperature. The same process was repeated as in the first wash. For the third and last washes, 250 µl of IVT Wash Buffer was added and centrifuged at 11,000g for 2 min at room temperature. After removing the flow through and placing the column back into a new 1.5 ml micro centrifuge tube, 20 µl of RNase free water was added directly onto the silica membrane of the spin column and incubated for 1 minute at room temperature. It was centrifuged at 11,000g for 1 min at room temperature and the purified sgRNA was

collected. The yield of sgRNA was determined using 2 µl to measure the OD using a nano drop spectrophotometer.

2.5 PCR Amplification of Target DNA

Using the Guide-it sgRNA Screening Kit, purified sgRNAs screening was performed for effective cleavage of their targets. Forward and reverse primers to amplify the tetracycline resistant regions targeted by CRISPR/Cas9 were designed. The optimal amplicon size is 600–800 bp, with the sgRNA target sequence located asymmetrically within the amplicon and each cleavage fragment was at least 250 bp, and not greater than >100 bp size difference between the fragments after Cas9 cleavage (Figure 9). The guidelines were to ensure efficient amplification and good assay resolution.

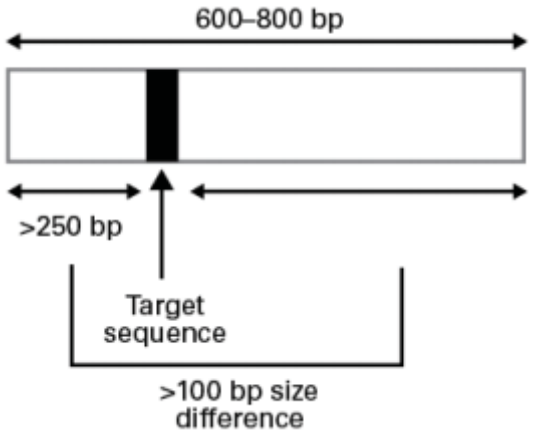

Figure 9: PCR amplicon design.

Table 3: sgRNA template forward and reverse primers for cas9 cleavage assay.

sgRNA Template	Forward Primer	Reverse Primer
T1	TACAGAAATGTATACTTCAATAAATGG	AAAACAGATTTTACAGTCCGTCA

T2	AATAAAAATTACAGAAATGTATACTTCA	TTACAGTCCGTCACATTCC
T3	AAATCTCAGATAGTGATCCGC	GAATGACCTCATTATTTTTCAATTGA
T5	AATATAGGGATTGATAACCTTATAGA	GTGAATGGTATATTCTGCATTTT
T6	ATGGAAGTGATTAGTGCACT	CTGTTAAACAAACACTACGTCCA

Following the Guide-it screening recipe and protocol, the PCR was done in 50 µL reactions using 10 µl of 2X Terra PCR Direct Buffer (with Mg^{2+}, dNTP) ,1.5 µL of Forward primer (10 µM) ,1.5 µL of Reverse primer (10 µM),1 µL of Terra PCR Direct Polymerase Mix (1.25 U/µl) ,19 µL of RNase Free Water, and 2 µL of genomic DNA from *Staphylococcus aureus subsp. aureus* (ATCC 700699DQ). The reactions were allowed to run in a preheated thermal cycler with an initial denaturation at 98 °C for 2 minutes, followed by 30 cycles of the following; denaturation at 98 °C for 10 seconds, annealing at 60 °C for 15 seconds, and extension at 68 °C for 1 minute/kb. The product (5 µL) was then run on a 1.2 % agarose gel.

2.6 Cas9 Cleavage Assay

According to the Guide-it invitro kit recipe and protocol, the sgRNA/cas9 complex was prepared in 1.5 µL reaction using 1 µl of Target-specific sgRNA (50 ng/µl) or control sgRNA (50 ng/µl) and 0.5µL of Guide-it Recombinant Cas9 Nuclease (500 ng/µl). The reaction was mixed very well by pipetting and incubated using a thermal cycler at 37 °C for 5 minutes. Then, the Cas9 assay was performed in 15 µL reactions using 5 µL of PCR reaction solution (100–250 ng) or control fragment, 1 µL of 15 X Cas9 Reaction Buffer ,1 µL of 15 X BSA 6.5 µL RNase free water and 1.5 µL Cas9/sgRNA mix. The reaction was

mixed very well by pipetting and incubated using a thermal cycler at 37 °C for 1 hour and 80 °C for 5 minutes. After incubation, 4 µL of nucleic acid dye was added to the sample and then loaded on a 1.2 % agarose gel. A 100bp ladder was also loaded onto the gel before starting the run.

2.7 Labeling of sgRNA

The sgRNA was labelled according to the ULYSIS Nucleic acid Labeling kit protocol (Thermofisher) with minimum optimization. The labeling dye in the kit used was Alexa Fluor 488 dye. 2 µL ULYSIS labeling reagent and labeling buffer was added to 1 µg of sgRNA to bring the final volume of reaction to 25 µL. The reaction was incubated at 85 °C for 15 minutes and then plunged into an ice bath and centrifuged briefly to redeposit the sample to the bottom of the tube. The labeled-sgRNA was purified from excess ULYSIS labeling reagent using a gel filtration –based spin column, according to the manufacturer's protocol (Bio-Rad Micro Bio-Spin P-30). The labelled nucleic acid was analyzed using the nucleic acid micro array function on the nano drop, and labeling efficiency was calculated.

3. Preparation of Antibody-conjugated Graphene Oxide (Ab-GO)

For the preparation of Ab-GO with 1 µg of dCas9 antibody, some stock reagents were prepared and they include 500 mM MES buffer (pH 4.0), 20 mM PBS buffer (pH 7.4), 2 % BSA in 20 mM PBS buffer (pH 7.4) and 1 mg/mL GO in 5 mM MES. Antibody-conjugated GO was synthesized by a classic two-step EDC-NHS (1-Ethyl-3 -(3-dimethylaminopropyl) carbodiimide and N-hydroxysuccinimide) method. Briefly, 1 mL of 20 µg/mL GO was ultrasonically dispersed in 5 mM of 2-(N-Morpholino) ethanesulfonic

acid (MES) buffer (pH=4.0) for 10 minutes. Then a MES buffer solution containing 4 mg/mL of EDC and 6 mg/mL of NHS was added into the GO-dispersed MES solution to activate the GO. The mixture was first stirred for 30 min at 15 °C, then centrifuged at 13000Xg and washed with 20 mM of phosphate buffer solution (PBS, pH=7.4) 3 times to remove unreacted coupling reagents. Then 1 µL of 1mg/ml dcas9 antibody was added to 99 µL 20 mM PBS buffer (pH 7.4). The activated GO was redispersed in 100 µL PBS dCas9 antibody solution to react with 1µg of dCas9 antibody so as to modify the GO with the antibody. The samples were mixed on an electronic shaker at 15 °C for 2 hours. Remaining active sites of GO were blocked with 2 % BSA in 20 mM PBS buffer solution for 30 min. The solution was then centrifuged at 13,000Xg for 10 min to remove any unbound biomolecules in the supernatant. Prepared antibody-conjugated graphene oxide was stored at 4 °C prior to characterization with AFM.

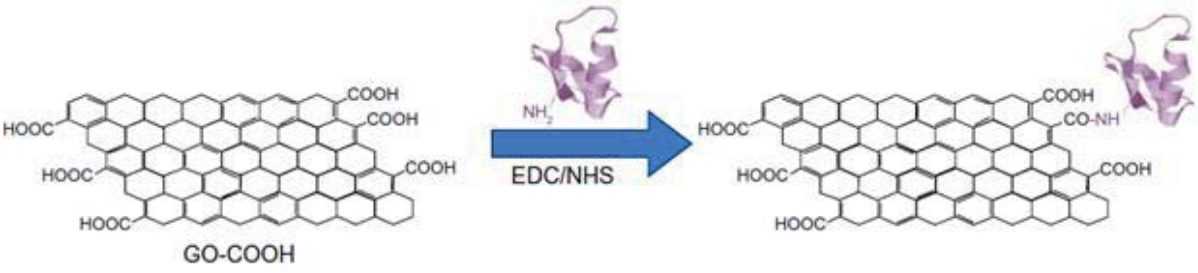

Figure 10: Schematic showing conjugation of Anti-CRISPR Cas9 antibody onto graphene oxide (GO).

3.1 **Characterization Method**

The bare GO, EDC: NHS activated GO and Antibody conjugated GO were characterized by atomic force microscopy (AFM) individually to determine if Ab-GO was prepared successfully. For AFM measurements, sample solutions containing bare GO or modified

GO were dripped on freshly cleaved glass surface using a pipette and then dried in ambient air. Surface topographic features were scanned in contact mode using a commercial AFM (CSPM4000, Benyuan, China) equipped with a silicon cantilever.

4. Ab-GO Sensitivity Assay

To perform this assay for sensitivity, we require the duplex buffer for the effective formation of the sgRNA/dCas9 complex. Also, SPECTRA max 190 Microplate Spectrophotometer was used for all incubation conditions while Biotek Synergy H1 microplate reader (Gen5 software) was used to measure florescence intensity. Four duplicate wells were used for protein only, no DNA, 1 nM gDNA and 10 nM gDNA samples. The total volume for each of the eight wells was 200 µL and the final concentrations of each component were 15.82 nM dCas9, 11.66 nM labeled-sgRNA, 2 µg/mL Ab-GO, and the genomic DNA samples of 1 nM and 10 nM. Basically, on a clean corning 96-well plate, duplex buffer was added followed by a 2 µg/mL final concentration of Ab-GO and dCas9 to each of the wells in that order respectively. The reaction was incubated for 30 min at 37 °C. At the end of the first incubation, labelled-sgRNA was added to the dCas9/Ab-GO complex and incubated again for 30 min at 37 °C to form the ribonucleoprotein duplex on the GO platform. Then the genomic DNA were added to the reactions, and incubated for 20 min at 37 °C. The Florescence intensity and emission spectrum was determined by a plate reader. Because we used Alexa 488 dye, the florescence was measured at 490 nm (excitation) and 525 nm (emission). Optical measurements were performed under ambient condition at room temperature. All data was collected in duplicate and average fluorescence intensity as well as standard deviation were calculated.

CHAPTER III – RESULTS AND DISCUSSION

1. Cloning and Purification

The dcas9 DNA sequence from a dcas9 plasmid (pdCas9) was cloned into pET_22b+ plasmid, a protein expression vector. This was performed by Genscript ((Piscataway, New Jersey) and the DNA sequence information are provided in the supplementary data. The restriction enzymes used are XhoI (CTCGAG) and NcoI (CCATGG) shown on the pET22b+ vector (Fig. 9). The expression vector has a His-tag DNA which was used for dcas9 purification via nickel column affinity chromatography.

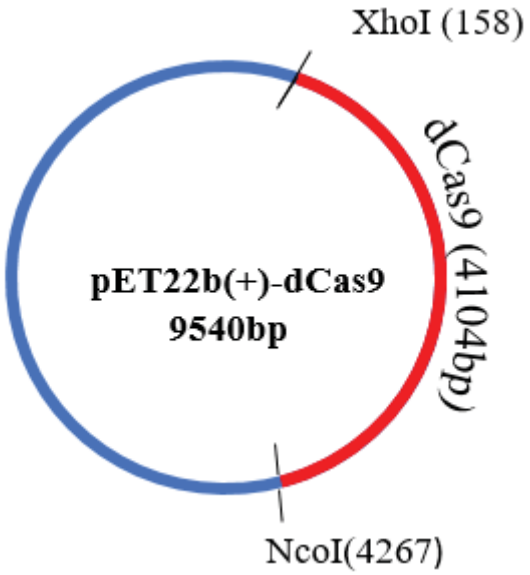

Figure 11: pET22b (+)-dCas9 Vector Map

After purification of dCas9, SDS-PAGE analysis was performed to determine the purity of proteins and molecular weight. Using the ProtParam tool (https://web.expasy.org/protparam/), the molecular weight of dcas9 was determined to be about 158 kDa. As indicated in the gel image below, the expected band corresponding to 158kDa can be seen underlined in yellow. Most of the unwanted proteins present in the

SDS-PAGE were removed in the fractions after purification with the nickel column. This was done by using a 100 kDa filter.

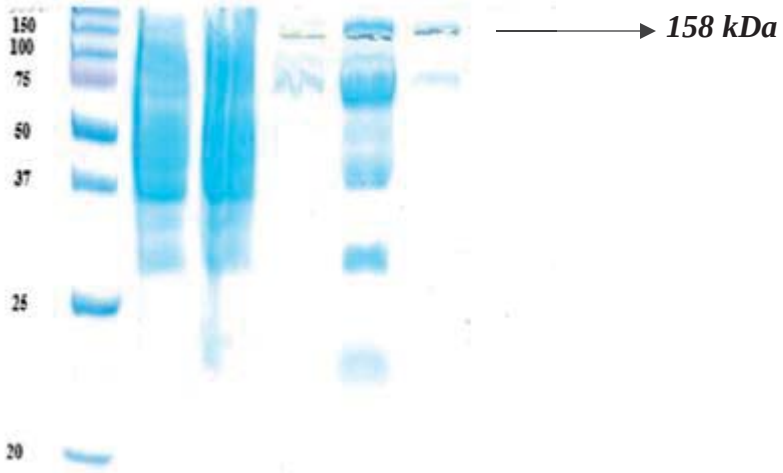

Figure 12: dCas9 SDS-PAGE image. The dCas9 protein ($\sim 158\ kDa$) band is indicated by an arrow on the right.

2. sgRNA design

The table below shows the result of an optimized sgRNA design to maximize activity and minimize off-target effects of CRISPR-dCas9. The sgRNAs were designed to target NGG protospacer adjacent motif (PAM)- containing sequences in both the positive and negative strands of the tetM gene. As shown in the table, only one target sequence is in the negative strand of tetM while the other four sequences are targeted toward the positive strand of the gene. These five sequences were selected based on their high specificity and efficiency scores as determined from the bench-ling CRISPR online tool (https://www.benchling.com/). Higher scores for both specificity and efficiency are better as it increases on-targeting and minimizes off-targeting effects.[35]

Table 4: Specificity and efficiency scores of the selected sgRNAs after design.

Position	Strand	N20 Sequence	PAM	Specificity Score	Efficiency Score
1113	1	TCCGCTTCTACGATATTACG	TGG	97.51868	65.89592
1103	-1	TCCACGTAATATCGTAGAAG	CGG	94.39204	56.10995
1339	1	TCTGTATCACCGCTTCCGTT	GGG	93.94427	55.07762
909	1	AATCGATAAGGCTTATTCCG	GGG	91.51745	68.63273
1426	1	GTTATGGAAGGGATACGCTA	TGG	90.64115	59.58768

2.1 Synthesis of sgRNA Template

To detect the tetM gene, six sgRNAs were optimally designed to reduce off-target binding. The sgRNA_4 was not included because its forward primer forms hairpin structure that inhibits amplification. This is one of the reasons we designed and selected more than one sgRNA. Another reason is to determine which of them have the best specificity during dcas9 sensitivity experiments. Also, for the purpose of multiplex detection, more than one sgRNAs will be required. In synthesizing these sgRNAs, the DNA template strands of each of them were amplified using PCR. According to the Guide-it invitro transcription kit protocol, a 130 bp band on an agarose gel should confirm that the sgRNA templates were correctly amplified. The result in Fig. 13 shows that the five sgRNA templates were correctly amplified. After amplifying the DNA template for sgRNA, an in vitro transcription was performed to synthesize sgRNA, which was screened for its binding

efficiency and specificity to target the tetM sequences. Thus, a DNA cleavage assay was performed to verify the sgRNAs.

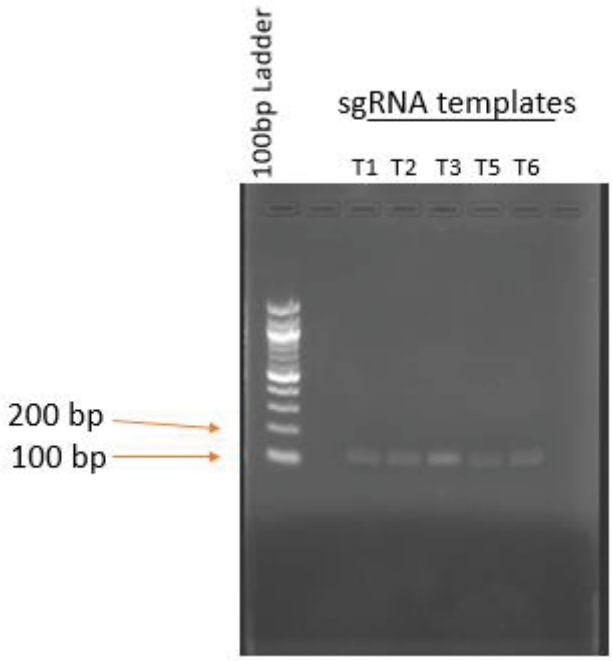

Fig 13: sgRNA Template Gel Image. Five sgRNA templates (T1, T2, T3, T5, AND T6) were synthesized and the approximately~130bp band was expected as shown in the agarose gel image above.

2.2 Cas9 cleavage assay before labeling

An *S.aureus* genomic DNA containing the tetM sequences was amplified to a 630 bp DNA fragment that was used for the Cas9 cleavage assay. Upon screening of the synthesized sgRNAs, the 630 bp DNA fragment was cleaved to 370 bp and 260 bp unequal fragments as shown on the gel image in Fig. 14. This result confirms that we successfully synthesized sgRNAs that can specifically bind to their targeted tetM sequences and thus, in complex with dCas9, could be used for DNA sensitivity assays. However, sgRNA_5 on lane 7 (Fig. 14) didn't generate any cleaved fragments upon binding the 630 bp DNA. In

theory, from the specificity and efficiency scores, we would expect a positive outcome from sgRNA_5 screening, but there was a low efficiency in the cleavage. This was the only exception among the five sgRNAs and further explains why we designed more than one sgRNAs. The percentage of gel used was 1.2 %.

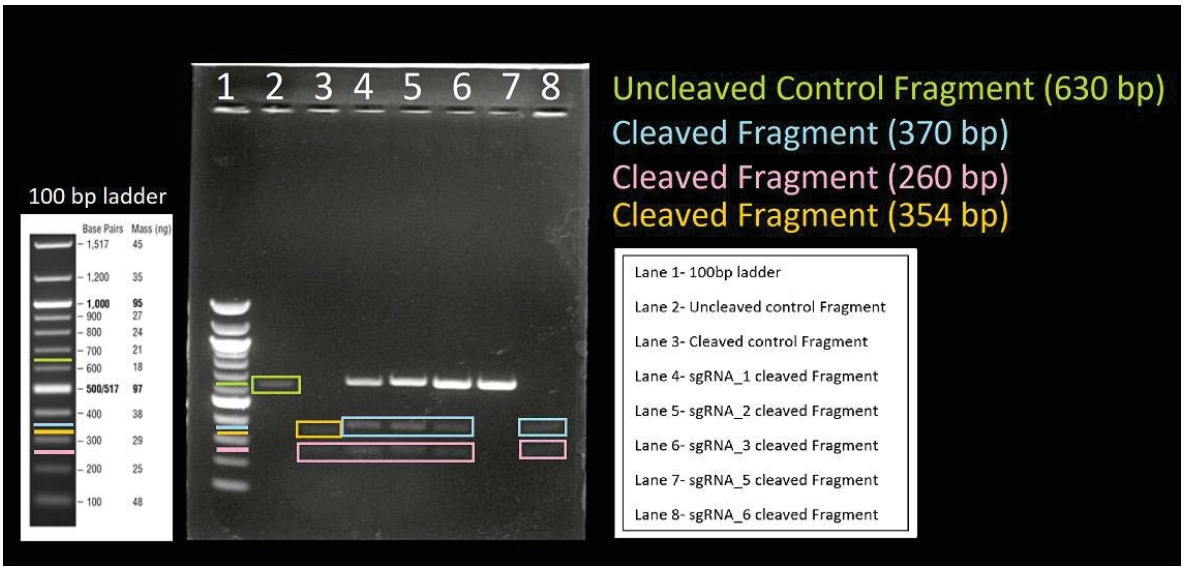

Fig 14: Cas9 Cleavage assay gel image before sgRNA labeling.

2.3 Cas9 cleavage assay after labeling

To perform florescence assays with dcas9/sgRNA to determine target DNA sensitivity and specificity, the sgRNAs were labelled with Alexa dye and further screened by Cas9 cleavage assay to ensure that the labelled-sgRNAs specificity to target was intact. The gel image in Fig. 15 shows the cleaved 370 bp and 260 bp unequal fragments indicating that Alexa _sgRNA can bind specifically to its target sequence. This data implies that effectively labeled Alexa-sgRNA can be used for dcas9/sgRNA_ Alexa florescence-based assay. The percentage of gel used was 1.2 %.

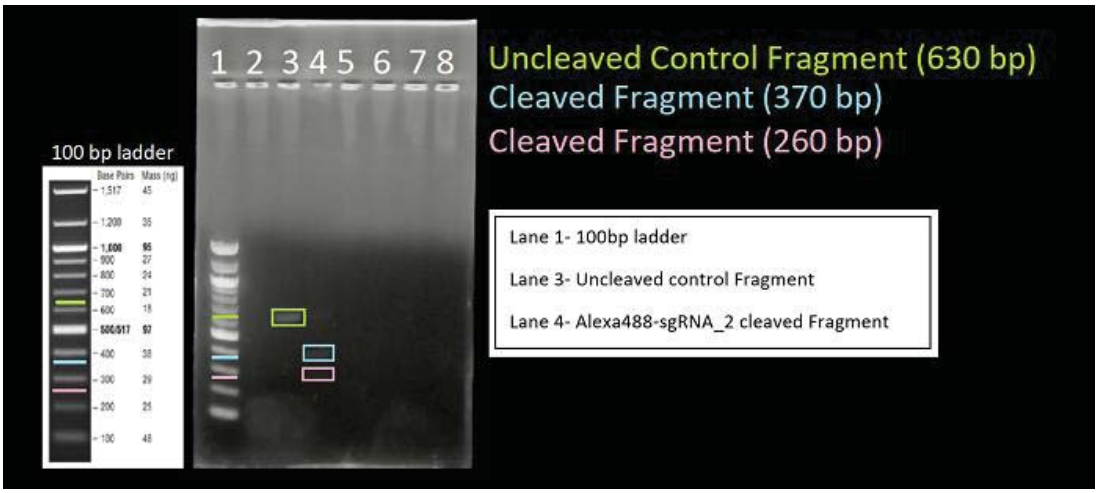

Fig 15: Cas9 Cleavage assay gel image after sgRNA labeling.

This is the follow up cleavage assay which shows the successful cleavage of the A488 labeled sgRNA_2 from the previous gel. The labeled sgRNA_2 was used because it showed a clear, bright bands of cleaved fragment and has a higher concentration than sgRNA_1. The labeling was successful and so was the follow up cleavage assay, showing that labeled sgRNA can bind to its target sequence without any loss in specificity due to the Alexa_488 dye.

2.4 Alexa-labeled sgRNA

After labeling sgRNA, we had to ensure that the sgRNA used is effectively labeled for florescence assays by calculating the labeling ratio as described in the Alexa ULYSIS kit protocol. The concentrations and the absorbance values of Alexa-sgRNA and Alexa dye are given in Table 5. The labeling ratio calculation procedure and calculated values are also shown for the Alexa_ sgRNAs under Table 6. According to the ULYSIS kit manual, an acceptable labeling ratio is in the range of 43-67 and this is what formed the basis of the Alexa_ sgRNA used for dCas9/sgRNA_ Alexa sensitivity assay.

Table 5: Alexa-sgRNA Nanodrop data.

Labelled-sgRNA	Concentration	A260(Abs)	260/280	Factor	Dye Abs	Dye Conc.
sgRNA_1	274.6 ng/µl	0.733	2.17	40.00	0.114	16.0 µM
sgRNA_2	176.0 ng/µl	0.448	2.25	40.00	0.010	1.3 µM
sgRNA_3	218.0 ng/µl	0.567	2.15	40.00	0.042	6.0 µM
sgRNA_6	99.7 ng/µl	0.267	2.18	40.00	0.042	5.9 µM

Table 6: Labeling ratios of the different sgRNAs. The acceptable range is between 43-67.

sgRNA	Abase (Corrected Absorbance)	Labeling Ratio
sgRNA_1	0.698	46
sgRNA_2	0.445	334
sgRNA_3	0.445	99.2
sgRNA_6	0.2544	45.5

Labeling Ratio = (Abase × εdye) / (Adye × εbase). Where,

Abase = A260 – (Adye × CF260), where,

Abase: corrected absorbance

CF260: correction factor = 0.30.

εdye = 62,000

εbase = 8250

As shown in Table 1, only four sgRNAs were labeled because their Cas9 cleavage assay screening was positive. Among the four samples of sgRNAs labeled, only sgRNA_1 and sgRNA_6 were successfully labeled because their values were within the range 43-67. The samples containing sgRNA_2 and sgRNA_3 had the labeling ratio values of 334 and 99.2, which are not within the acceptable range. Those high values indicate that the nucleic

acid to dye ratio was low and need to be optimized. For the florescence sensitivity assay, Alexa- sgRNA_1 was frequently used because it was higher in concentration and had the better labeling ratio than Alexa- sgRNA_6. Also, Alexa- sgRNA_1 was preferred because its target 630 bp genomic DNA had a much better yield than that of Alexa- sgRNA_6.

3. CRISPR- based Ab-GO DNA detection

As a proof of concept, Alexa-labelled sgRNA_1/dcas9 was used to detect the tetM targeted sequence complementary to the N20-sequence of the guide RNA. This study demonstrated a novel CRISPR-/Ab-GO DNA detection system. This approach was validated for the detection of the antibiotic resistant gene tetM. GO was successfully conjugated with the anti-CRISPR Cas9 antibody, to immobilize dCas9 protein, and then the surface morphology was characterized to confirm the antibodies bound to GO.

3.1 Surface Morphologies of GO by AFM

Atomic force microscopy (AFM) was introduced to measure the various stages of the surface modification of GO. According to Huang et al., the height of GO would obviously increase after being activated by EDC-NHS and further upon conjugation by antibodies.[36] This study served as a reference point for us to use AFM to characterize the surface morphologies of bare GO, EDC-NHS-activated GO, and antibody-conjugated GO to provide evidence of the EDC-NHS coupling reaction and the presence of antibodies on the GO surface. In Fig. 15(a), bare GO has a thin and flat appearance with a height of approximately 4 nm on the glass slide, which may correspond to the monolayer state of GO. The corresponding line scan and height profile of the sample is shown in Fig. 15(b). After activation by EDC-NHS, GO exhibits an increased thickness of about 8 nm. The line

scan (arrow) gives a corresponding cross-sectional height profile in Fig. 16 (b), showing an uniform surface of the GO. Because the antibody is very large (with a molecular weight of over 150 kDa, one can correctly expect that the antibody-conjugated GO should be much thicker. As shown in Fig. 16 (a), we observed that the height of antibody-conjugated GO increased dramatically, with a typical thickness of about 12 nm, as suggested in the height profile in Fig. 16 (b). Some bright peaks were observed on this sample, which was also similar to the report of Huang et al.[36] The bright peaks are most likely due to the accumulation of antibodies on the GO surface. All of the surface morphology results implied that the antibody was successfully retained on the GO surface.

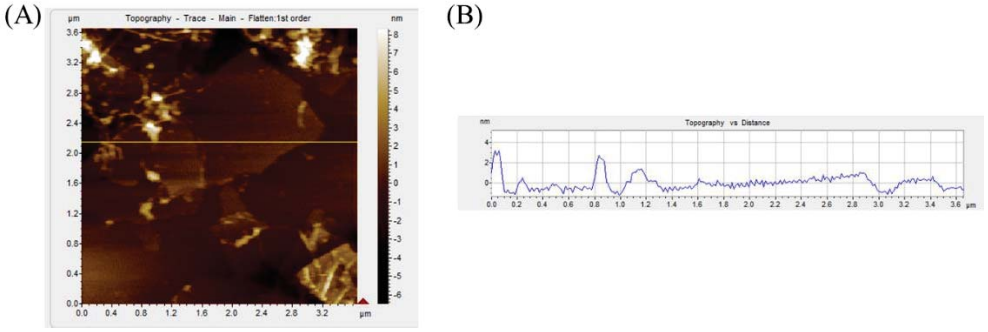

Figure 16. (A): Surface morphology of bare GO by AFM on a freshly cleaved glass slide (1.2 μm×1.3 μm). (B): Height profile of the line scans (arrows) in Bare GO (3-6 nm).

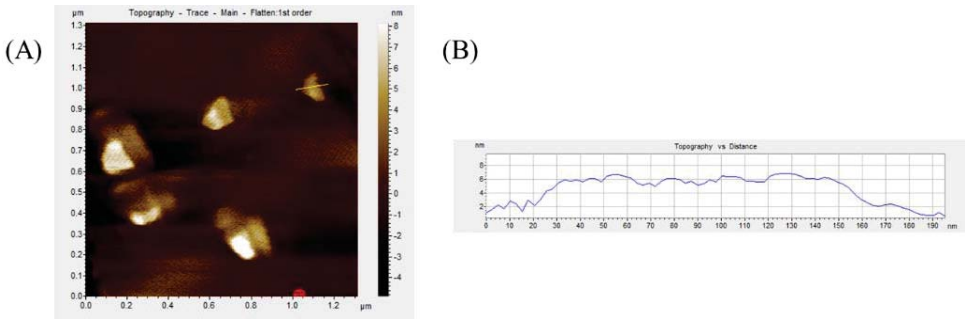

Figure 17 (A): Surface morphology of Activated GO by AFM on a freshly cleaved glass slide (1.2 µm×1.3 µm) (B): Height profiles of the line scans (arrows) in EDC-NHS activated GO (5-8 nm).

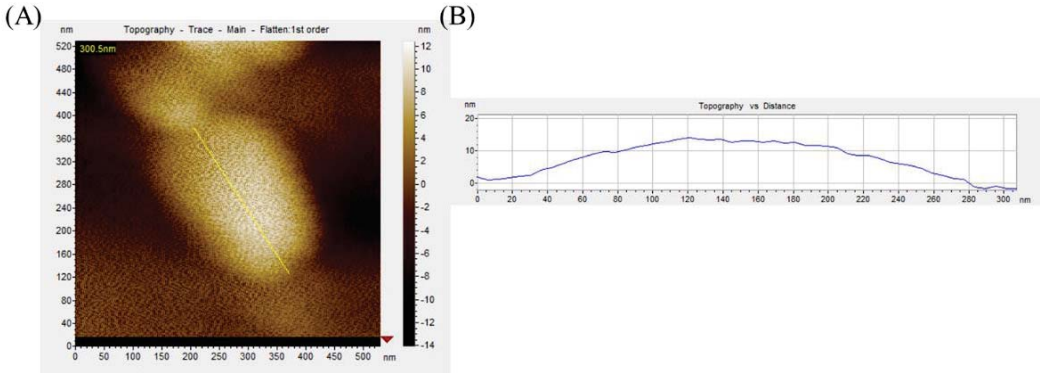

Figure 18 (A): Surface morphology of Activated Ab-GO by AFM on a freshly cleaved glass slide (1.2 µm×1.3 µm) (B): Height profiles of the line scans (arrows) in antibody conjugated GO (8-14 nm).

3.2 Specificity of CRISPR/dCas9

Our approach was examined to determine the specificity of Alexa-sgRNA/dCas9 complex in the presence of target and non-target DNAs. Our target DNA sequence in the tetM gene was target site 6 (T6) while the non-target sequence, also present in the tetM gene, was target site 1 (T1). The irrelevant DNA sequence was ZifHSO dsDNA oligonucleotides and its sequence is not present in the tetM gene. As shown in Fig. 10, when an Alexa-sgRNA_6/dCas9 complex was incubated with its own target DNA (T1), the signal was distinctly higher than those of non-target and irrelevant DNAs as we expected.

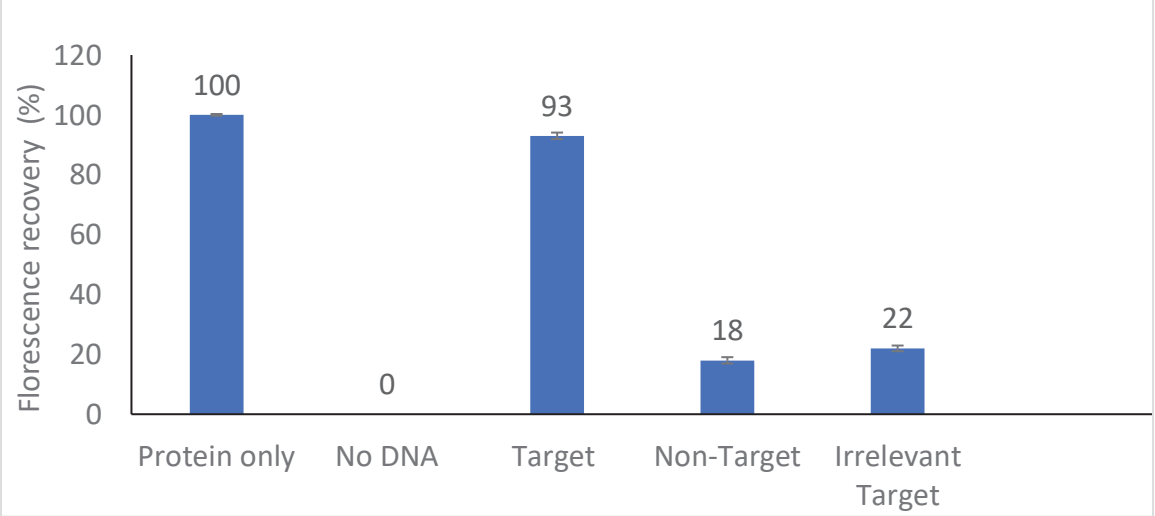

Figure 19: The specificity of Alexa-sgRNA_6/dCas9 complex; Fluorescence intensity of Alexa-labeled dCas9/sgRNA-6 after incubation with tetM_6 (target), tetM_1 (non-target), and ZifHSO (irrelevant target) dsDNAs. The concentrations of Ab-GO were 2 µg/µl and dsDNAs were 10 nM. Error bars represent the standard deviation of the mean.

3.2 Sensitivity

To validate our Alexa-labelled CRISPR/dcas9 complex and Ab-GO approach, two concentrations of target DNA, 1nM and 10 nM were utilized in our FRET-based assay to determine the sensitivity of our system. Our sensitivity data (Figure 7) confirms that our novel approach can be used for detecting DNA. To calculate percent recovery of fluorescence signal, the equation below was used where $F_{0\ is}$ florescence intensity at the maxima in the absence of GO, F_1 is the fluorescence intensity at the maxima in the presence of GO, and Fi is the fluorescence intensity at the maxima in the presence of target DNA:

% Fluorescence recovery = $100 - \frac{Fo-Fi}{Fo-F1}$ x 100

The fluorescence intensity recovery was 18% at 1 nM of DNA, which was determined to be the limit of detection. Because of the 18 % recovery at 1 nM, we anticipate that DNA detection can be achieved at lower concentrations with some florescence recovery. Upon addition of 10 nM DNA, the florescence recovery increased to 50%, which is more than two times the florescence recovery at 1nM. This confirms that an increase in DNA concentrations will result in greater dissociation of the CRISPR/dcas9 complex from the Ab-GO, and in turn a greater florescence signal.

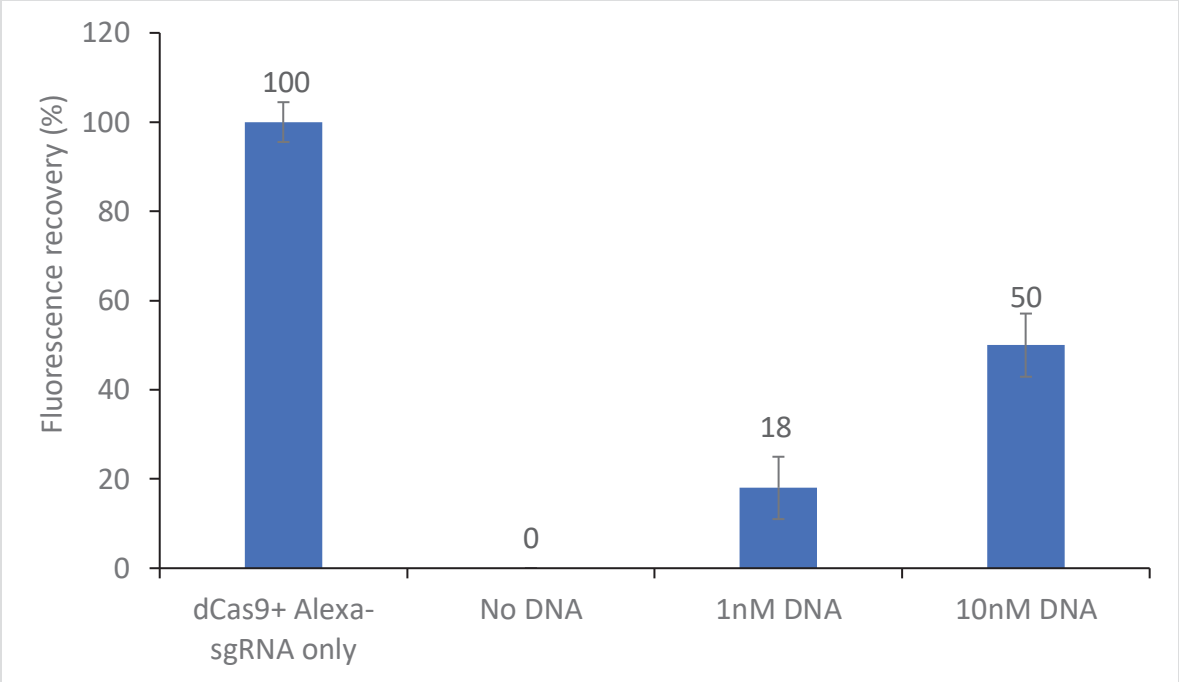

Figure 20: The limit of detection of the dCas9/Alexa-sgRNA_1 at 1 nM.

There are other methods based on dcas9/sgRNA that have been used for DNA detection with the greater sensitivity than our approach.[10,20,32] In this study, we have demonstrated a proof of concept of a novel DNA detection system with promising potentials for DNA detection at high sensitivity. Thus, the high sensitivity, specificity, and reliability of RNA-guided CRISPR/Cas nuclease-based nucleic acid detection shows great promise for the development of next-generation molecular diagnostics technology.[37] Also, further optimizations on AB-GO conjugation and dcas9 expression and purification, our limit of detection can be improved in the femtomolar range similar to the graphene field effect transistor (gFET) approach, which produced a 1.7fM limit of detection.[32] It was reported that a dcas9/sgRNA approach-based DNA denaturation and subsequent hybridization can be used for the detection of Methicillin resistant staphylococcus aureus (MRSA) antibiotic resistant gene.[20] But, our approach can be used for the direct detection

of dsDNA without DNA denaturation or target DNA Labeling. Recently, many nucleic acid detection methods are combined with isothermal amplification methods, such as recombinase polymerase amplification (RPA), and loop-mediated isothermal amplification (LAMP).[37] However, the separate nucleic acid pre-amplification and multiple manual operations required by these CRISPR-Cas-based detection methods undoubtedly complicate the procedures and bring about contaminations whereas our system does not require any preamplification steps. Apart from the incubation time of 30 minutes each to immobilize dcas9 and sgRNA respectively, our assay requires 15 minutes for DNA detection. There is even a possibility that DNA detection could occur at shorter time considering the optimizations on-going experiments to improve this new method. With further development, our detection approach can be suitably utilized for a point of care diagnostic application unlike PCR-based methods which are time- and cost-consuming, requiring expensive equipment and well-trained personnel.

CHAPTER IV – CONCLUSIONS

In this study, we have demonstrated the direct detection of the pathogen-specific genomic dsDNA sequence utilizing complementary sgRNA in complex with dcas9 immobilized on an antibody-conjugated graphene oxide (Ab-GO). Our novel detection approach can provide a facile, rapid and sensitive technology without several laborious steps involved in DNA denaturation, and subsequent hybridization, and DNA-labeling. Our dCas9/sgRNA complex showed adequate sensitivity toward its own target DNA, suggesting that the ribonucleoprotein immobilized on Ab-GO could be further developed into a novel and reliable molecular device for pathogen detection. In the future, we will focus on improving the sensitivity by exploring methods to enhance dcas9 conjugation to GO, and sgRNA labeling. For example, quantum dots can be labelled on sgRNA as an alternative to organic dyes. We are currently working on an optimized procedure for obtaining a high yield of purified dcas9 in order to perform further assays including specificity and GO quenching assays. Then, we will move on to perform multiplex detection of different pathogenic dsDNA by utilizing different sgRNAs. We also anticipate to determine the sensitivity, and specificity of our system to detect cell lysates of antibiotic resistant bacterial. In this study, our sensing system was able to detect target DNA from a whole genomic DNA sample containing a lot of non-target DNA sequences. Our system could also be used as a lab-on-a-chip diagnostic by integrating our technology with a microfluidic component to pre-concentrate cell lysates and improve limit of detection.[38] In summary, we have demonstrated that GO-based CRISPR/dcas9/sgRNA approach can specifically bind to its target DNA sequence within the tetM gene. Unlike ZFPs and TALEs, sgRNA design is based on complementary target DNA sequence for more specific

binding and targeting without requiring any modular engineering of dcas9 protein. Thus, our method is based on the most recent DNA diagnostic technology.

SUPPLEMENTARY DATA

Red indicates D10A and H840A mutations in dCas9 gene.

i. dCas9_pET22b (+) Vector

atggataagaaatatagcatcggtctg**gcg**attggcaccaacagcgtgggttgggcggttatcaccgacgagtacaaagtgccg
agcaagaaatttaaggttctgggcaacaccgatcgtcacagcatcaagaaaaacctgattggtgcgctgctgtttgacagcggtg
aaaccgcggaagcgacccgtctgaaacgtaccgcgcgtcgtcgttacacccgtcgtaagaaccgtatctgctacctgcaggag
attttcagcaacgaaatggcgaaggtggacgatagcttctttcaccgtctggaggaaagcttcctggttgaggaagataagaaac
acgagcgtcacccgatctttggtaacattgtggacgaggttgcgtatcacgaaaaatacccgaccatctatcacctgcgtaagaa
actggtggacagcaccgataaagcggacctgcgtctgatctatctggcgctggcgcacatgattaagttccgtggtcactttctga
tcgaaggcgatctgaacccggacaacagcgatgtggacaagctgttcatccagctggttcaaacctacaaccagctgtttgagg
aaaacccgattaacgcgagcggtgttgacgcgaaagcgatcctgagcgcgcgtctgagcaagagccgtcgtctggagaacct
gatcgcgcaactgccgggtgaaaagaaaaacggtctgtttggcaacctgattgcgctgagcctgggcctgaccccgaacttcaa
gagcaactttgatctggcggaggacgcgaaactgcagctgagcaaggacacctatgacgatgacctggataacctgctggcgc
aaatcggcgatcagtacgcggacctgttcctggcggcgaaaaacctgagcgacgcgatcctgctgagcgatattctgcgtgtga
acaccgagattaccaaagcgccgctgagcgcgagcatgatcaagcgttatgacgaacaccaccaagatctgaccctgctgaag
gcgctggttcgtcagcaactgccggagaagtacaaggaaatcttctttgatcaaagcaagaacggttacgcgggctatattgacg
gtggcgcgagccaggaagagttctacaagtttatcaaaccgattctggagaagatggacggtaccgaggaactgctggtgaaa
ctgaaccgtgaagacctgctgcgtaagcaacgtacctttgataacggtagcatcccgcaccagattcatctgggtgaactgcat**g**
cgatcctgcgtcgtcaggaagacttctacccgtttctgaaagataaccgtgagaagatcgaaaaaattctgaccttccgtattccgt
actatgttggtccgctggcgcgtggcaacagccgttttgcgtggatgacccgtaaaagcgaggaaaccatcaccccgtggaact
tcgaggaagtggttgataagggcgcgagcgcgcaaagcttcattgagcgtatgaccaactttgacaaaaacctgccgaacgaa
aaagtgctgccgaagcacagcctgctgtacgagtatttcaccgtttataacgaactgaccaaggtgaaatacgttaccgagggta
tgcgtaagccggcgttcctgagcggcgaacaaaagaaagcgatcgtggacctgctgtttaaaaccaaccgtaaggtgaccgtta
agcagctgaaagaggactacttcaagaaaattgaatgcttcgatagcgtggagatcagcggtgttgaagaccgttttaacgcgag
cctgggcacctaccacgatctgctgaagatcattaaggataaagacttcctggacaacgaggaaaacgaggatatcctggaaga
cattgtgctgaccctgaccctgtttgaggatcgtgaaatgatcgaggaacgtctgaaaacctatgcgcacctgttcgatgacaagg
ttatgaaacagctgaagcgtcgtcgttacaccggttggggccgtctgagccgtaagctgatcaacggtattcgtgacaaacaaag
cggcaagaccattctggactttctgaaaagcgatggtttcgcgaaccgtaactttatgcagctgattcacgatgacagcctgacctt
caaagaggatatccagaaggcgcaagttagcggtcaaggcgacagcctgcacgaacatattgcgaacctggcgggtagccc
ggcgatcaagaaaggcattctgcagaccgtgaaagtggttgacgagctggtgaaagttatgggtcgtcacaagccggaaaaca
tcgttattgagatggcgcgtgaaaaccagaccacccaaaaaggccagaagaacagccgtgagcgtatgaaacgtatcgagga
aggtattaaggaactgggcagccagatcctgaaagagcacccggtggaaaacacccagctgcaaaacgagaagctgtatctgt
actatctgcaaaacggtcgtgatatgtacgttgaccaggaactggatattaaccgtctgagcgattacgacgtggatgcgatcgtt
ccgcaaagcttcctgaaagatgacagcattgacaacaaggtgctgacccgtagcgacaaaaaccgtggcaagagcgataacg
ttccgagcgaggaagtggttaagaaaatgaagaactactggcgtcaactgctgaacgcgaaactgatcacccagcgtaagtttg
ataacctgaccaaagcggagcgtggtggcctgagcgaactggacaaagcgggtttcattaagcgtcaactggtggagacccgt
cagatcaccaaacacgttgcgcagattctggatagccgtatgaacaccaagtacgatgagaacgacaaactgatccgtgaagtg
aaggttattaccctgaagagcaaactggttagcgacttccgtaaggatttccaattctacaaggttcgtgaaatcaacaactatcac
cacgcgcacgacgcgtacctgaacgcggtggttggtaccgcgctgattaagaaatacccgaaactggagagcgaattcgtgta

cggcgactataaggtgtacgatgttcgtaaaatgatcgcgaagagcgagcaggaaattggtaaagcgaccgcgaagtatttcttt
tacagcaacatcatgaacttctttaagaccgagatcaccctggcgaacggtgaaatccgtaagcgtccgctgattgagaccaacg
gcgagaccggcgaaatcgtgtgggacaaaggccgtgattttgcgaccgtgcgtaaggttctgagcatgccgcaagtgaacatt
gttaagaaaaccgaggttcagaccggtggcttcagcaaggaaagcattctgccgaaacgtaacagcgataagctgatcgcgcg
taagaaagactgggatccgaagaaatatggtggcttcgacagcccgaccgtggcgtacagcgttctggtggttgcgaaggtgg
agaagggtaaaagcaagaaactgaaaagcgttaaggaactgctgggcatcaccattatggagcgtagcagcttcgagaagaa
cccgatcgattttctggaggcgaaaggttataaggaagtgaagaaagacctgatcattaaactgccgaagtacagcctgtttgag
ctggaaaacggccgtaaacgtatgctggcgagcgcgggcgagctgcagaaaggcaacgaactggcgctgccgagcaagta
cgtgaacttcctgtatctggcgagccactacgagaagctgaaaggtagcccggaggataacgaacagaaacaactgtttgttga
gcaacacaagcactatctggacgagatcattgaacagattagcgaattcagcaaacgtgtgatcctggcggacgcgaacctgg
ataaggttctgagcgcgtacaacaaacaccgtgataagccgatccgtgagcaggcggaaaacatcattcacctgttcaccctga
ccaacctgggtgcgccggcggcgttcaaatattttgacaccaccattgatcgtaaacgttacaccagcaccaaagaggtgctgg
acgcgaccctgatccaccaaagcattaccggcctgtacgaaacccgtatcgacctgagccagctgggtggcgat

ii. dCas9.dna

atggataagaaatatagcatcggtctg**gcg**attggcaccaacagcgtgggttgggcggttatcaccgacgagtacaaagtgccg
agcaagaaatttaaggttctgggcaacaccgatcgtcacagcatcaagaaaaacctgattggtgcgctgctgtttgacagcggtg
aaaccgcggaagcgacccgtctgaaacgtaccgcgcgtcgtcgttacacccgtcgtaagaaccgtatctgctacctgcaggag
attttcagcaacgaaatggcgaaggtggacgatagcttctttcaccgtctggaggaaagcttcctggttgaggaagataagaaac
acgagcgtcacccgatctttggtaacattgtggacgaggttgcgtatcacgaaaaatacccgaccatctatcacctgcgtaagaa
actggtggacagcaccgataaagcggacctgcgtctgatctatctggcgctggcgcacatgattaagttccgtggtcactttctga
tcgaaggcgatctgaacccggacaacagcgatgtggacaagctgttcatccagctggttcaaacctacaaccagctgtttgagg
aaaacccgattaacgcgagcggtgttgacgcgaaagcgatcctgagcgcgcgtctgagcaagagccgtcgtctggagaacct
gatcgcgcaactgccgggtgaaaagaaaaacggtctgtttggcaacctgattgcgctgagcctgggcctgaccccgaacttcaa
gagcaactttgatctggcggaggacgcgaaactgcagctgagcaaggacacctatgacgatgacctggataacctgctggcgc
aaatcggcgatcagtacgcggacctgttcctggcggcgaaaaacctgagcgacgcgatcctgctgagcgatattctgcgtgtga
acaccgagattaccaaagcgccgctgagcgcgagcatgatcaagcgttatgacgaacaccaccaagatctgaccctgctgaag
gcgctggttcgtcagcaactgccggagaagtacaaggaaatcttctttgatcaaagcaagaacggttacgcgggctatattgacg
gtggcgcgagccaggaagagttctacaagtttatcaaaccgattctggagaagatggacggtaccgaggaactgctggtgaaa
ctgaaccgtgaagacctgctgcgtaagcaacgtacctttgataacggtagcatcccgcaccagattcatctgggtgaactgcat**g**
cgatcctgcgtcgtcaggaagacttctacccgtttctgaaagataaccgtgagaagatcgaaaaaattctgaccttccgtattccgt
actatgttggtccgctggcgcgtggcaacagccgttttgcgtggatgacccgtaaaagcgaggaaaccatcaccccgtggaact
tcgaggaagtggttgataagggcgcgagcgcgcaaagcttcattgagcgtatgaccaactttgacaaaaacctgccgaacgaa
aaagtgctgccgaagcacagcctgctgtacgagtatttcaccgtttataacgaactgaccaaggtgaaatacgttaccgagggta
tgcgtaagccggcgttcctgagcggcgaacaaaagaaagcgatcgtggacctgctgtttaaaaccaaccgtaaggtgaccgtta
agcagctgaaagaggactacttcaagaaaattgaatgcttcgatagcgtggagatcagcggtgttgaagaccgttttaacgcgag
cctgggcacctaccacgatctgctgaagatcattaaggataaagacttcctggacaacgaggaaaacgaggatatcctggaaga
cattgtgctgaccctgaccctgtttgaggatcgtgaaatgatcgaggaacgtctgaaaacctatgcgcacctgttcgatgacaagg
ttatgaaacagctgaagcgtcgtcgttacaccggttggggccgtctgagccgtaagctgatcaacggtattcgtgacaaacaaag
cggcaagaccattctggactttctgaaaagcgatggtttcgcgaaccgtaactttatgcagctgattcacgatgacagcctgacctt
caaagaggatatccagaaggcgcaagttagcggtcaaggcgacagcctgcacgaacatattgcgaacctggcgggtagccc

ggcgatcaagaaaggcattctgcagaccgtgaaagtggttgacgagctggtgaaagttatgggtcgtcacaagccggaaaaca
tcgttattgagatggcgcgtgaaaaccagaccacccaaaaaggccagaagaacagccgtgagcgtatgaaacgtatcgagga
aggtattaaggaactgggcagccagatcctgaaagagcacccggtggaaaacacccagctgcaaaacgagaagctgtatctgt
actatctgcaaaacggtcgtgatatgtacgttgaccaggaactggatattaaccgtctgagcgattacgacgtggatgcgatcgtt
ccgcaaagcttcctgaaagatgacagcattgacaacaaggtgctgacccgtagcgacaaaaaccgtggcaagagcgataacg
ttccgagcgaggaagtggttaagaaaatgaagaactactggcgtcaactgctgaacgcgaaactgatcacccagcgtaagtttg
ataacctgaccaaagcggagcgtggtggcctgagcgaactggacaaagcgggtttcattaagcgtcaactggtggagacccgt
cagatcaccaaacacgttgcgcagattctggatagccgtatgaacaccaagtacgatgagaacgacaaactgatccgtgaagtg
aaggttattaccctgaagagcaaactggttagcgacttccgtaaggatttccaattctacaaggttcgtgaaatcaacaactatcac
cacgcgcacgacgcgtacctgaacgcggtggttggtaccgcgctgattaagaaatacccgaaactggagagcgaattcgtgta
cggcgactataaggtgtacgatgttcgtaaaatgatcgcgaagagcgagcaggaaattggtaaagcgaccgcgaagtatttcttt
tacagcaacatcatgaacttctttaagaccgagatcaccctggcgaacggtgaaatccgtaagcgtccgctgattgagaccaacg
gcgagaccggcgaaatcgtgtgggacaaaggccgtgattttgcgaccgtgcgtaaggttctgagcatgccgcaagtgaacatt
gttaagaaaaccgaggttcagaccggtggcttcagcaaggaaagcattctgccgaaacgtaacagcgataagctgatcgcgcg
taagaaagactgggatccgaagaaatatggtggcttcgacagcccgaccgtggcgtacagcgttctggtggttgcgaaggtgg
agaagggtaaaagcaagaaactgaaaagcgttaaggaactgctgggcatcaccattatggagcgtagcagcttcgagaagaa
cccgatcgattttctggaggcgaaaggttataaggaagtgaagaaagacctgatcattaaactgccgaagtacagcctgtttgag
ctggaaaacggccgtaaacgtatgctggcgagcgcgggcgagctgcagaaaggcaacgaactggcgctgccgagcaagta
cgtgaacttcctgtatctggcgagccactacgagaagctgaaaggtagcccggaggataacgaacagaaacaactgtttgttga
gcaacacaagcactatctggacgagatcattgaacagattagcgaattcagcaaacgtgtgatcctggcggacgcgaacctgg
ataaggttctgagcgcgtacaacaaacaccgtgataagccgatccgtgagcaggcggaaaacatcattcacctgttcaccctga
ccaacctgggtgcgccggcggcgttcaaatattttgacaccaccattgatcgtaaacgttacaccagcaccaaagaggtgctgg
acgcgaccctgatccaccaaagcattaccggcctgtacgaaacccgtatcgacctgagccagctgggtggcgat

iii. dCas9 Amino acid sequence

MDKKYSIGLAIGTNSVGWAVITDEYKVPSKKFKVLGNTDRHSIKKNLIGALLFDSGETAE
ATRLKRTARRRYTRRKNRICYLQEIFSNEMAKVDDSFFHRLEESFLVEEDKKHERHPIFG
NIVDEVAYHEKYPTIYHLRKKLVDSTDKADLRLIYLALAHMIKFRGHFLIEGDLNPDNSD
VDKLFIQLVQTYNQLFEENPINASGVDAKAILSARLSKSRRLENLIAQLPGEKKNGLFGNL
IALSLGLTPNFKSNFDLAEDAKLQLSKDTYDDDLDNLLAQIGDQYADLFLAAKNLSDAIL
LSDILRVNTEITKAPLSASMIKRYDEHHQDLTLLKALVRQQLPEKYKEIFFDQSKNGYAG
YIDGGASQEEFYKFIKPILEKMDGTEELLVKLNREDLLRKQRTFDNGSIPHQIHLGELHAI
LRRQEDFYPFLKDNREKIEKILTFRIPYYVGPLARGNSRFAWMTRKSEETITPWNFEEVVD
KGASAQSFIERMTNFDKNLPNEKVLPKHSLLYEYFTVYNELTKVKYVTEGMRKPAFLSG
EQKKAIVDLLFKTNRKVTVKQLKEDYFKKIECFDSVEISGVEDRFNASLGTYHDLLKIIKD
KDFLDNEENEDILEDIVLTLTLFEDREMIEERLKTYAHLFDDKVMKQLKRRRYTGWGRL
SRKLINGIRDKQSGKTILDFLKSDGFANRNFMQLIHDDSLTFKEDIQKAQVSGQGDSLHE
HIANLAGSPAIKKGILQTVKVVDELVKVMGRHKPENIVIEMARENQTTQKGQKNSRERM
KRIEEGIKELGSQILKEHPVENTQLQNEKLYLYYLQNGRDMYVDQELDINRLSDYDVDAI
VPQSFLKDDSIDNKVLTRSDKNRGKSDNVPSEEVVKKMKNYWRQLLNAKLITQRKFDN
LTKAERGGLSELDKAGFIKRQLVETRQITKHVAQILDSRMNTKYDENDKLIREVKVITLK
SKLVSDFRKDFQFYKVREINNYHHAHDAYLNAVVGTALIKKYPKLESEFVYGDYKVYD

VRKMIAKSEQEIGKATAKYFFYSNIMNFFKTEITLANGEIRKRPLIETNGETGEIVWDKGR
DFATVRKVLSMPQVNIVKKTEVQTGGFSKESILPKRNSDKLIARKKDWDPKKYGGFDSP
TVAYSVLVVAKVEKGKSKKLKSVKELLGITIMERSSFEKNPIDFLEAKGYKEVKKDLIIKL
PKYSLFELENGRKRMLASAGELQKGNELALPSKYVNFLYLASHYEKLKGSPEDNEQKQL
FVEQHKHYLDEIIEQISEFSKRVILADANLDKVLSAYNKHRDKPIREQAENIIHLFTLTNLG
APAAFKYFDTTIDRKRYTSTKEVLDATLIHQSITGLYETRIDLSQLGGD

BIBLOGRAPHY

1. Bengtsson-Palme, J.; Kristiansson, E.; Larsson, D. G. J., *Fems Microbiology Reviews* **2018,** *42* (1), 68-80.

2. Collignon, P., *Internal medicine journal* **2015,** *45* (11), 1109-1115.

3. So, A. D.; Shah, T. A.; Roach, S.; Chee, Y. L.; Nachman, K. E., *Journal of Law Medicine & Ethics* **2015,** *43*, 38-45.

4. Berendonk, T. U.; Manaia, C. M.; Merlin, C.; Fatta-Kassinos, D.; Cytryn, E.; Walsh, F.; Burgmann, H.; Sorum, H.; Norstrom, M.; Pons, M. N.; Kreuzinger, N.; Huovinen, P.; Stefani, S.; Schwartz, T.; Kisand, V.; Baquero, F.; Martinez, J. L., *Nature Reviews Microbiology* **2015,** *13* (5), 310-317.

5. Martínez, J. L.; Coque, T. M.; Baquero, F., *Nature reviews. Microbiology* **2014,** *13* (2), 116-123.

6. Cao, L.; Cui, X. Y.; Hu, J.; Li, Z. D.; Choi, J. R.; Yang, Q. Z.; Lin, M.; Ying, H. L.; Xu, F., *Biosensors & Bioelectronics* **2017,** *90*, 459-474.

7. Batista, A. C.; Pacheco, L. G. C., *Journal of Microbiological Methods* **2018,** *152*, 98-104.

8. Kim, M. S.; Kini, A. G., *Molecules and Cells* **2017,** *40* (8), 533-541.

9. Kellner, M. J.; Koob, J. G.; Gootenberg, J. S.; Abudayyeh, O. O.; Zhang, F., *Nature Protocols* **2019,** *14* (10), 2986-3012.

10. Koo, B.; Kim, D. E.; Kweon, J.; Jin, C. E.; Kim, S. H.; Kim, Y.; Shin, Y., *Sensors and Actuators B-Chemical* **2018,** *273*, 316-321.

11. Doudna, J. A.; Charpentier, E., *Science* **2014,** *346* (6213), 1077-+.

12. Kim, H.; Kim, J.-S., *Nature reviews. Genetics* **2014,** *15* (5), 321-334.

13. Makarova, K. S.; Wolf, Y. I.; Alkhnbashi, O. S.; Costa, F.; Shah, S. A.; Saunders, S. J.; Barrangou, R.; Brouns, S. J. J.; Charpentier, E.; Haft, D. H.; Horvath, P.; Moineau, S.; Mojica, F.

J. M.; Terns, R. M.; Terns, M. P.; White, M. F.; Yakunin, A. F.; Garrett, R. A.; van der Oost, J.; Backofen, R.; Koonin, E. V., *Nature Reviews Microbiology* **2015,** *13* (11), 722-736.

14. Jiang, F. G.; Taylor, D. W.; Chen, J. S.; Kornfeld, J. E.; Zhou, K. H.; Thompson, A. J.; Nogales, E.; Doudna, J. A., *Science* **2016,** *351* (6275), 867-871.

15. Yao, R. L.; Liu, D.; Jia, X.; Zheng, Y.; Liu, W.; Xiao, Y., *Synthetic and Systems Biotechnology* **2018,** *3* (3), 135-149.

16. Zhou, L.; Peng, R.; Zhang, R.; Li, J., *Journal of cellular and molecular medicine* **2018,** *22* (12), 5807-5815.

17. Zhou, W. H.; Hu, L.; Ying, L. M.; Zhao, Z.; Chu, P. K.; Yu, X. F., *Nature Communications* **2018,** *9*.

18. Huang, M. Q.; Zhou, X. M.; Wang, H. Y.; Xing, D., *Analytical Chemistry* **2018,** *90* (3), 2193-2200.

19. Gootenberg, J. S.; Abudayyeh, O. O.; Lee, J. W.; Essletzbichler, P.; Dy, A. J.; Joung, J.; Verdine, V.; Donghia, N.; Daringer, N. M.; Freije, C. A.; Myhrvold, C.; Bhattacharyya, R. P.; Livny, J.; Regev, A.; Koonin, E. V.; Hung, D. T.; Sabeti, P. C.; Collins, J. J.; Zhang, F., *Science (American Association for the Advancement of Science)* **2017,** *356* (6336), 438-442.

20. Guk, K.; Keem, J. O.; Hwang, S. G.; Kim, H.; Kang, T.; Lim, E. K.; Jung, J., *Biosensors & Bioelectronics* **2017,** *95*, 67-71.

21. Zhang, X. J.; Hu, Y.; Yang, X. T.; Tang, Y. Y.; Han, S. Y.; Kang, A.; Deng, H. S.; Chi, Y. M.; Zhu, D.; Lu, Y., *Biosensors & Bioelectronics* **2019,** *138*.

22. Wang, X. Y.; Yu, S. M.; Liu, W.; Fu, L. W.; Wang, Y. Q.; Li, J. H.; Chen, L. X., *Acs Sensors* **2018,** *3* (2), 378-385.

23. Charron, D. M.; Zheng, G., *Nano Today* **2018,** *18*, 124-136.

24. Kyrychenko, A.; Rodnin, M. V.; Ghatak, C.; Ladokhin, A. S., *Data in Brief* **2017,** *12*, 213-221.

25. Sidhu, J. S.; Singh, A.; Garg, N.; Singh, N., *ACS applied materials & interfaces* **2017,** *9* (31), 25847-25856.

26. Torchilin, V. P., *Nature reviews. Drug discovery* **2014,** *13* (11), 813-827.

27. Loh, K. P.; Bao, Q.; Eda, G.; Chhowalla, M., *Nature chemistry* **2010,** *2* (12), 1015-1024.

28. Dreyer, D. R.; Park, S.; Bielawski, C. W.; Ruoff, R. S., *Chemical Society reviews* **2010,** *39* (1), 228-240.

29. De, M.; Chou, S. S.; Dravid, V. P., *Journal of the American Chemical Society* **2011,** *133* (44), 17524-17527.

30. Chang, H.; Tang, L.; Wang, Y.; Jiang, J.; Li, J., *Analytical chemistry (Washington)* **2010,** *82* (6), 2341-2346.

31. Huang, A.; Li, W.; Shi, S.; Yao, T., *Scientific reports* **2017,** *7* (1), 40772-40772.

32. Hajian, R.; Balderston, S.; Tran, T.; DeBoer, T.; Etienne, J.; Sandhu, M.; Wauford, N. A.; Chung, J. Y.; Nokes, J.; Athaiya, M.; Paredes, J.; Peytavi, R.; Goldsmith, B.; Murthy, N.; Conboy, I. M.; Aran, K., *Nature Biomedical Engineering* **2019,** *3* (6), 427-437.

33. Qi, L. S.; Larson, M. H.; Gilbert, L. A.; Doudna, J. A.; Weissman, J. S.; Arkin, A. P.; Lim, W. A., *Cell* **2013,** *152* (5), 1173-1183.

34. *CRISPR: Methods and Protocols*. 2015 ed.; Springer New York: New York, NY, Vol. 1311.

35. Doench, J. G.; Fusi, N.; Sullender, M.; Hegde, M.; Vaimberg, E. W.; Donovan, K. F.; Smith, I.; Tothova, Z.; Wilen, C.; Orchard, R.; Virgin, H. W.; Listgarten, J.; Root, D. E., *Nature biotechnology* **2016,** *34* (2), 184-191.

36. Huang, A.; Zhang, L.; Li, W.; Ma, Z.; Shuo, S.; Yao, T., *Royal Society open science* **2018,** *5* (4), 171808-171808.

37. Xiong, D.; Kun, Y.; Ziyue, L.; Rajesh, V. L.; Enrique, B.; Maroun, M. S.; Changchun, L., *Nature communications* **2020,** *11* (1), 4711-4711.

38. Gao, N.; Gao, T.; Yang, X.; Dai, X. C.; Zhou, W.; Zhang, A. Q.; Lieber, C. M., *Proceedings of the National Academy of Sciences of the United States of America* **2016,** *113* (51), 14633-14638.